Osborn's Brain

IMAGING, PATHOLOGY, AND ANATOMY

SECOND EDITION

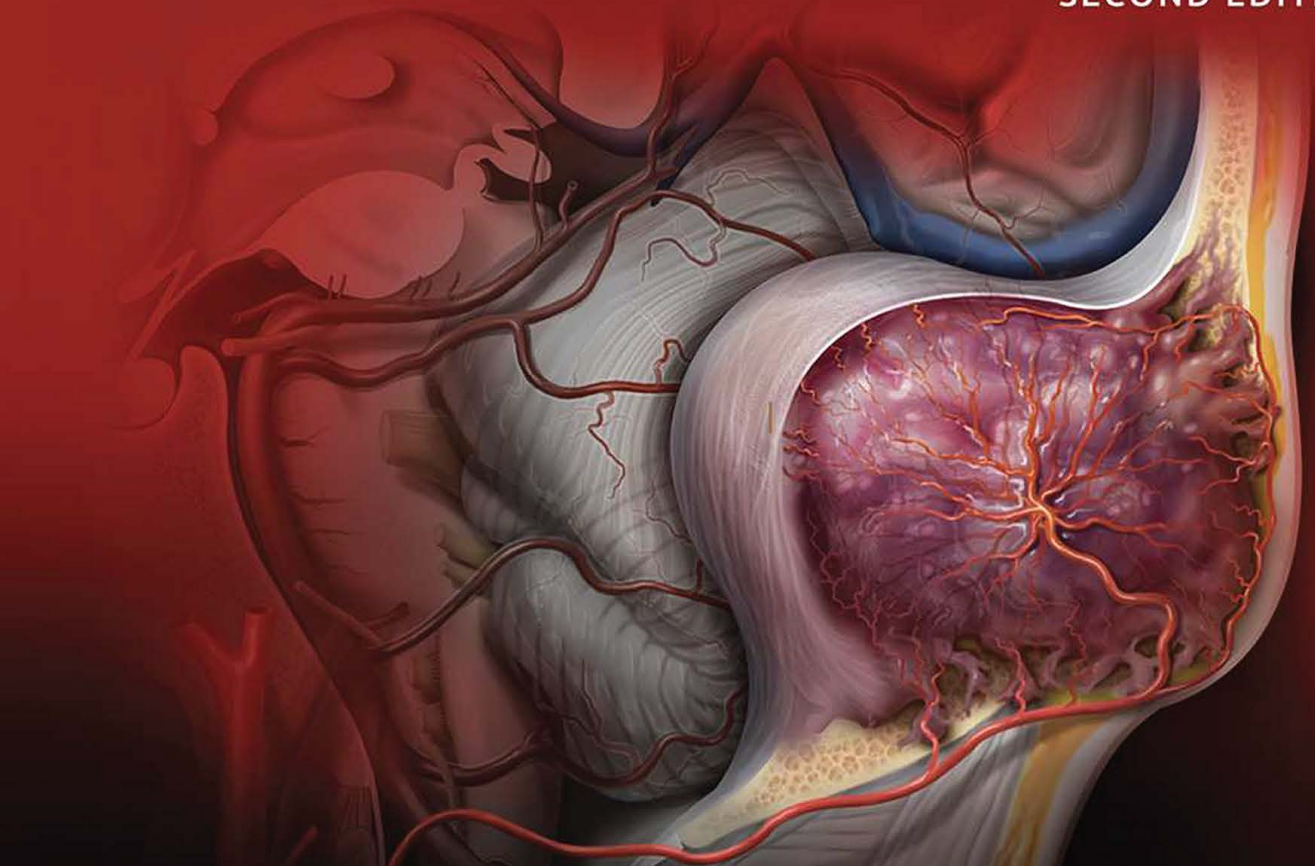

Anne G. Osborn
Hedlund | Salzman

ELSEVIER

Osborn's Brain

IMAGING, PATHOLOGY, AND ANATOMY

SECOND EDITION

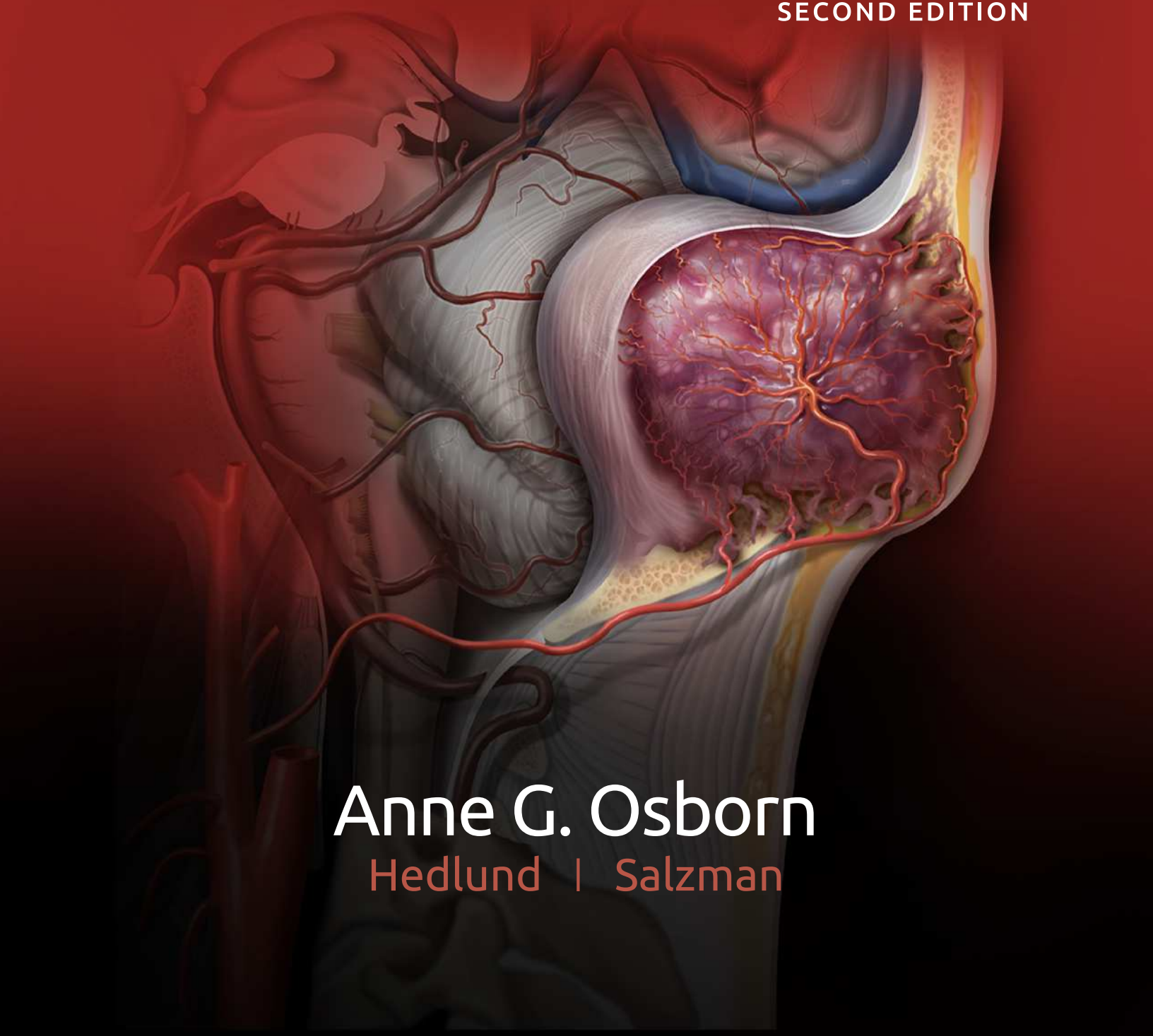

Anne G. Osborn

Hedlund | Salzman

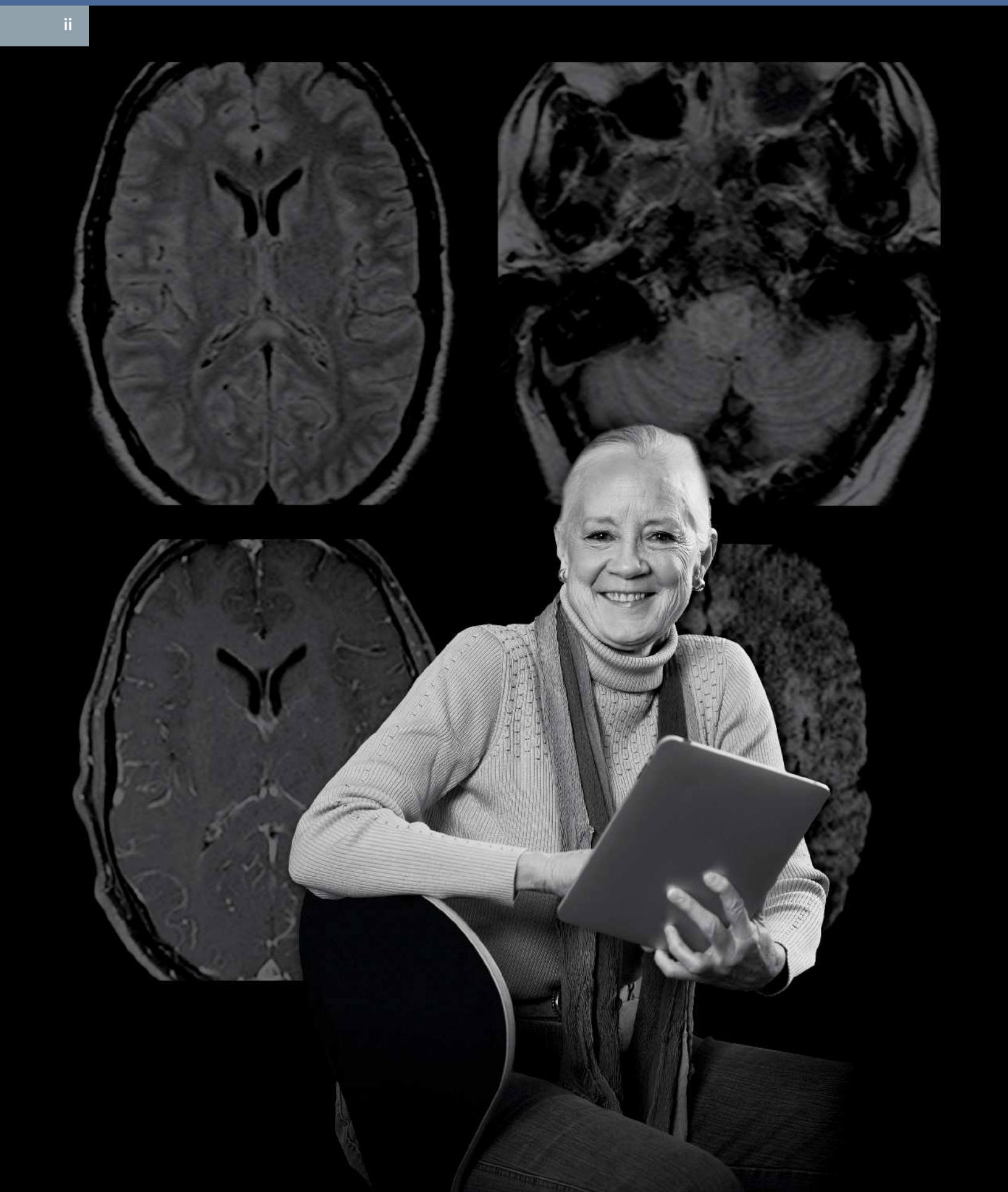

Osborn's Brain

IMAGING, PATHOLOGY, AND ANATOMY

SECOND EDITION

Anne G. Osborn, MD, FACR

University Distinguished Professor and Professor of Radiology and Imaging Sciences
William H. and Patricia W. Child Presidential Endowed Chair in Radiology
University of Utah School of Medicine
Salt Lake City, Utah

Gary L. Hedlund, DO

Pediatric Radiologist and Neuroradiologist
Primary Children's Hospital
Department of Medical Imaging
Intermountain Healthcare
Adjunct Professor of Radiology
University of Utah School of Medicine
Salt Lake City, Utah

Karen L. Salzman, MD

Professor of Radiology and Imaging Sciences
Neuroradiology Section Chief and Fellowship Director
Leslie W. Davis Endowed Chair in Neuroradiology
University of Utah School of Medicine
Salt Lake City, Utah

ELSEVIER

1600 John F. Kennedy Blvd.
Ste 1800
Philadelphia, PA 19103-2899

OSBORN'S BRAIN, SECOND EDITION ISBN: 978-0-323-47776-5

Notices

Knowledge and best practice in this field are constantly changing. As new research and experience broaden our understanding, changes in research methods, professional practices, or medical treatment may become necessary.

Practitioners and researchers must always rely on their own experience and knowledge in evaluating and using any information, methods, compounds, or experiments described herein. In using such information or methods they should be mindful of their own safety and the safety of others, including parties for whom they have a professional responsibility.

With respect to any drug or pharmaceutical products identified, readers are advised to check the most current information provided (i) on procedures featured or (ii) by the manufacturer of each product to be administered, to verify the recommended dose or formula, the method and duration of administration, and contraindications. It is the responsibility of practitioners, relying on their own experience and knowledge of their patients, to make diagnoses, to determine dosages and the best treatment for each individual patient, and to take all appropriate safety precautions.

To the fullest extent of the law, neither the Publisher nor the authors, contributors, or editors, assume any liability for any injury and/or damage to persons or property as a matter of products liability, negligence or otherwise, or from any use or operation of any methods, products, instructions, or ideas contained in the material herein.

Publisher Cataloging-in-Publication Data

Names: Osborn, Anne G., 1943-
Title: Osborn's brain / [edited by] Anne G. Osborn.
Description: Second edition. | Salt Lake City, UT : Elsevier, Inc., [2017] | Includes bibliographical references and index.
Identifiers: ISBN 978-0-323-47776-5
Subjects: LCSH: Brain--Pathophysiology--Handbooks, manuals, etc. | Central nervous system--Diseases--Handbooks, manuals, etc. | Brain--Imaging--Handbooks, manuals, etc. | MESH: Brain--physiopathology--Atlases. | Central Nervous System--pathology--Atlases. | Neuroimaging--methods--Atlases.
Classification: LCC RC386.5.O83 2017 | NLM WL 301 | DDC 616.8--dc23

International Standard Book Number: 978-0-323-47776-5
Cover Designer: Tom M. Olson, BA
Cover Art: Lane R. Bennion, MS

Printed in Canada by Friesens, Altona, Manitoba, Canada

Last digit is the print number: 9 8 7 6 5 4 3 2 1

Dedications

FOR RON

Beloved sweetheart, eternal companion, and soulmate, you didn't live to see the first edition completed and then watch it become an international bestseller. The second edition is even better, and I hope it makes you even more proud. I love you beyond expression and devote every day of my life in the service of others and in honor of your memory.

AO

FOR DIANA, AARON, AND JAIME

For Diana, my beloved, my best friend.
Your unwavering support nourishes my creative spirit. Thank you, sweetheart.
For Aaron, you honor the integrity of relationship and honest work. This inspires me.
For Jaime, your whole-hearted humanity illuminates the sacredness of our work in the service of others.

GLH

FOR MY FRIENDS AND COLLEAGUES IN NEURORADIOLOGY

To those of you at the University of Utah and around the world, thank you for the wonderful collaborations over the years. I am fortunate to practice in a field with such talented experts. My work is elevated because of your knowledge and support, for which I am in a constant state of gratitude.

KLS

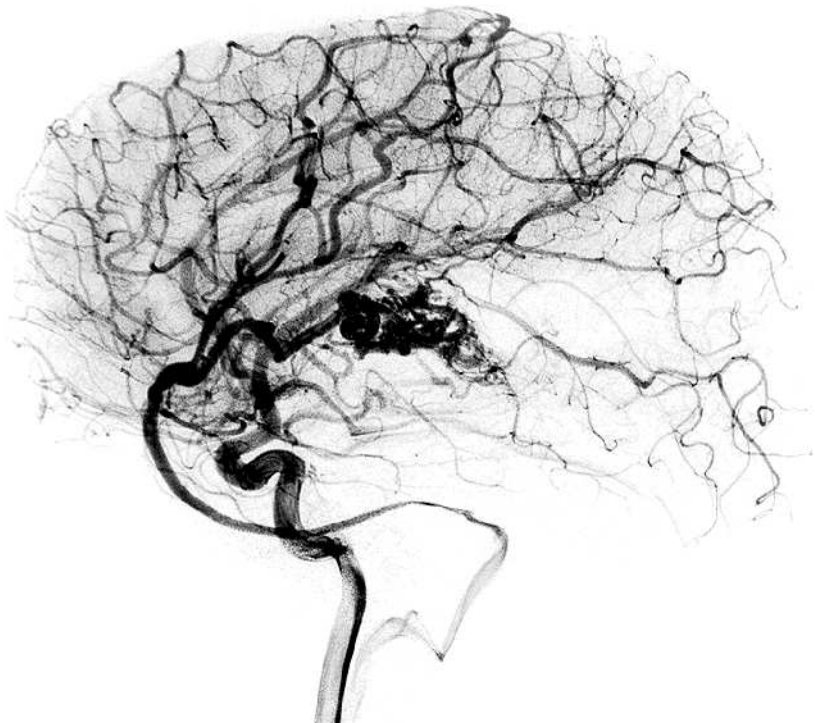

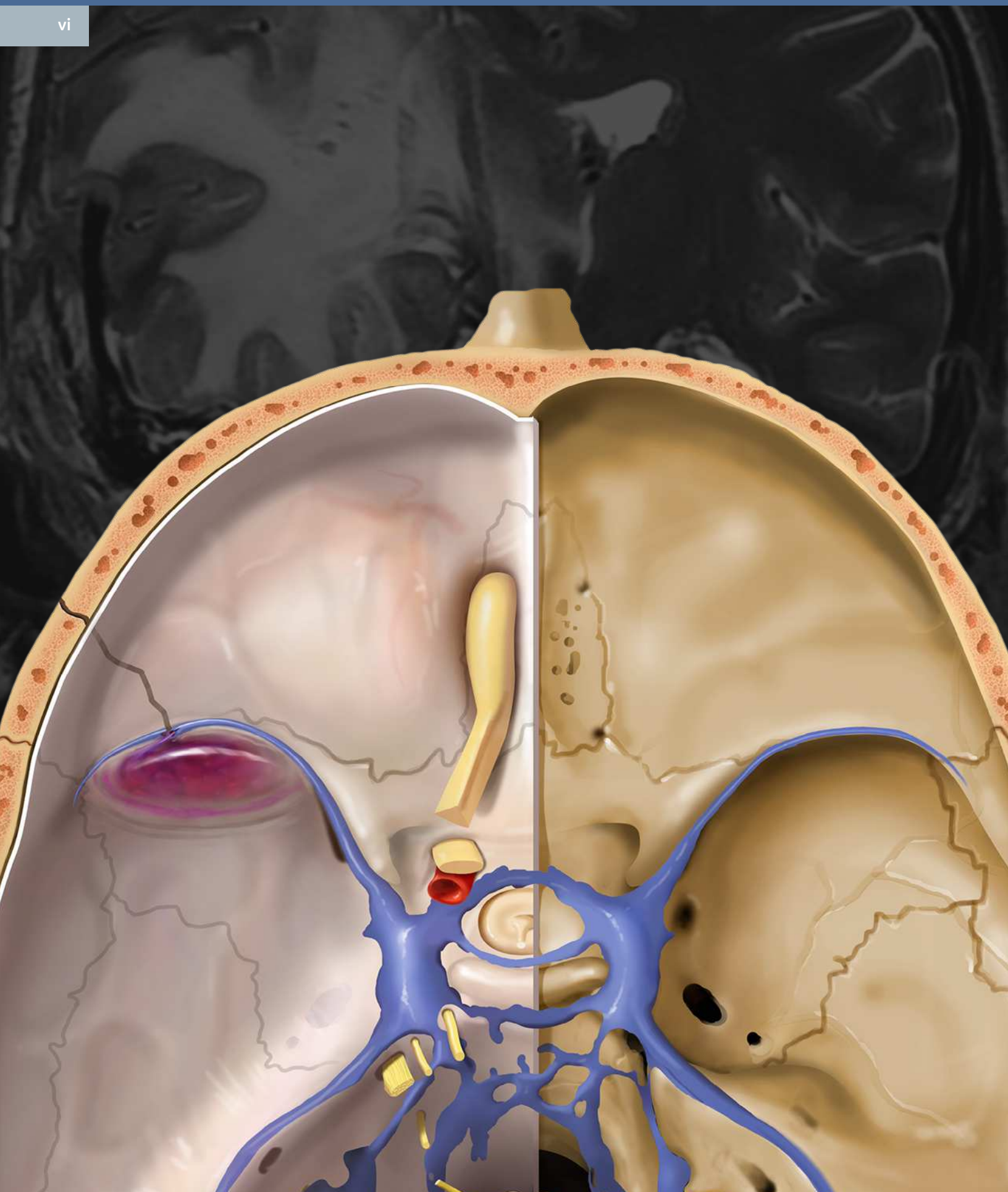

Preface

With *Osborn's Brain*, first edition, not only did I break a promise to myself that I would "never, EVER write another prose-based textbook," I would have been stunned to know I'd actually write a *second edition* of the book! But here we are, five years later, and I've done it. There have been so many changes in neuroradiology since the publication of the first edition that I wanted—and needed—to do a thorough update.

This edition is actually more than just an update; it is a major rewrite. Most of the 4,000+ images have been replaced with new, even better examples, and there are numerous new diagnoses that are presented. The Cancer Genome Atlas project has revolutionized our understanding of CNS neoplasms, and the exploding knowledge was reflected in the latest World Health Organization's *Classification of Tumours of the Central Nervous System*, published just a year ago. The "4-plus" WHO forms the basis of the completely rewritten neoplasms section of this edition.

For those of you who are new to *Osborn's Brain*, both the first and second editions are written as a curriculum in neuroradiology. The "must know—now!" topics such as brain trauma, stroke, and brain bleeds are covered in the first few chapters of the text. The book is meant to be read cover to cover, progressing through all the major areas of neuroimaging and neuropathology. While the basics are emphasized, there is a great deal of "advanced" information (read: fellow-and-beyond level stuff) that practicing neuroradiologists will find helpful and informative.

As with the first edition, this book is image-rich with hundreds of color graphics and gross pathology examples that inform the thousands of new, up-to-date images. I've expanded on my trademark summary "blue boxes" that are scattered throughout the text, allowing for a quick review of the essential facts.

Lastly, I invited two beloved colleagues, Drs. Gary Hedlund and Karen Salzman, to join me in authoring parts of the second edition. Gary is a revered pediatric neuroradiologist who is an international expert on (among other things) abusive head trauma. Karen's forte is tumor imaging, and her special focus is sella/parasellar disease. They are both highly respected members of our "Brain Team," and I have been privileged to work with them on this edition.

So as you start your journey through *Osborn's Brain*, second edition, best wishes and good reading to all of you! After all, you're why we write these things in the first place!

Anne G. Osborn, MD, FACR
University Distinguished Professor and Professor of Radiology and Imaging Sciences
William H. and Patricia W. Child Presidential Endowed Chair in Radiology
University of Utah School of Medicine
Salt Lake City, Utah

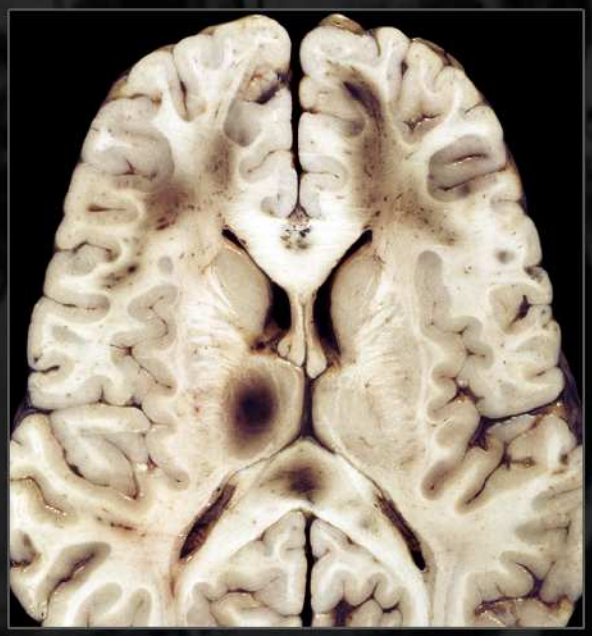

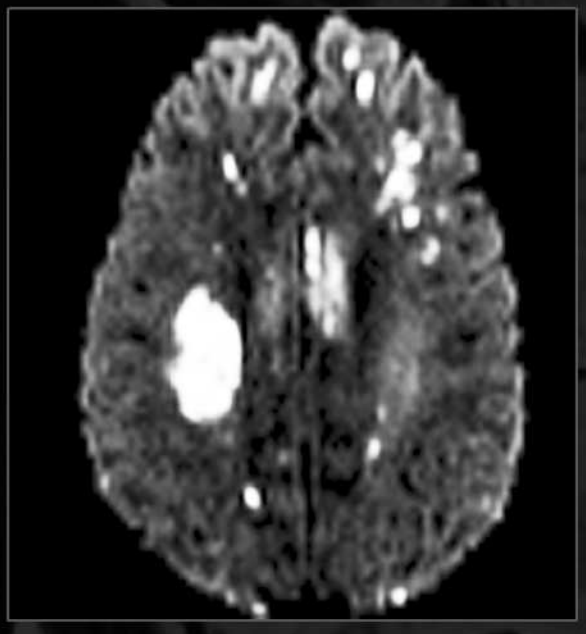

Image Contributors

AFIP Archives
D. P. Agamanolis, MD
N. Agarwal, MD
J. Ardyn, MD
M. Ayadi, MD
S. Aydin, MD
D. Bertholdo, MD
S. Blaser, MD
J. Boxerman, MD
M. Brant-Zawadski, MD
P. Burger, MD
S. Candy, MD
M. Castillo, MD
P. Chapman, MD
L. Chimelli, MD
S. Chung, MD
M. Colombo, MD
J. Comstock, MD
J. Curé, MD
B. Czerniak, MD
A. Datir, MD
B. N. Delman, MD
B. K. DeMasters, MD
K. Digre, MD
H. D. Dorfman, MD
M. Edwards-Brown, MD
D. Ellison, MD
H. Els, MD
A. Ersen, MD
W. Fang, MD
N. Foster, MD
C. E. Fuller, MD
S. Galetta, MD
C. Glastonbury, MBBS
S. Harder, MD
H. R. Harnsberger, MD
B. Hart, MD
E. T. Hedley-White, MD
G. Hedlund, DO
R. Hewlett, MD
P. Hildenbrand, MD
C. Y. Ho, MD
B. Horten, MD
C. Hsu, MD
M. Huckman, MD
P. Hudgins, MD
A. Illner, MD
B. Jones, MD
J. A. Junker, MD
E. C. Klatt, MD
D. Kremens, MD
W. Kucharczyk, MD
P. Lasjaunias, MD
S. Lincoff, MD
T. Markel, MD
M. Martin, MD
A. Maydell, MD
S. McNally, MD
T. Mentzel, MD
C. Merrow, MD
M. Michel, MD
K. Moore, MD
S. Nagi, MD
T. P. Naidich, MD
N. Nakase, MD
S. Narendra, MD
K. Nelson, MD
R. Nguyen, MD
G. P. Nielsen, MD
M. Nielsen, MS
K. K. Oguz, MD
J. P. O'Malley, MD
N. Omar, MD
J. Paltan, MD
G. Parker, MD
T. Poussaint, MD
R. Ramakantan, MD
C. Rambaud, MD
M. L. Rivera-Zengotita, MD
C. Robson, MBChB
F. J. Rodriguez, MD
P. Rodriguez, MD
A. Rosenberg, MD
E. Ross, MD
A. Rossi, MD
L. Rourke, MD
Rubinstein Collection, AFIP Archives
E. Rushing, MD
M. Sage, MD
B. Scheithauer, MD
P. Shannon, MD
A. Sillag, MD
E. T. Tali, MD
M. Thurnher, MD
T. Tihan, MD
K. Tong, MD
J. Townsend, MD
U. of Utah Dept. of Dermatology
S. van der Westhuizen, MD
M. Warmuth-Metz, MD
T. Winters, MD
A. T. Yachnis, MD
S. Yashar, MD

Acknowledgments

Editor in Chief

Karen E. Concannon, MA, PhD

Text Editors

Arthur G. Gelsinger, MA
Nina I. Bennett, BA
Terry W. Ferrell, MS
Lisa A. Gervais, BS
Matt W. Hoecherl, BS
Megg Morin, BA

Image Editors

Jeffrey J. Marmorstone, BS
Lisa A. M. Steadman, BS

Illustrations

Lane R. Bennion, MS
Richard Coombs, MS
Laura C. Wissler, MA
James A. Cooper, MD

Art Direction and Design

Tom M. Olson, BA
Laura C. Wissler, MA

Software Development and Support

Michael A. Hogenson, BS
Craig L. Moon, BS
Stephen Stephenson
Alma Miller

Production Coordinators

Rebecca L. Bluth, BA
Angela M. G. Terry, BA
Emily C. Fassett, BA

ELSEVIER

Table of Contents

Section 1:

Trauma

Section 2:

Nontraumatic Hemorrhage and Vascular Lesions

Section 3:

Infection, Inflammation, and Demyelinating Diseases

Table of Contents

Section 4:

Neoplasms, Cysts, and Tumor-Like Lesions

Section 5:

Toxic, Metabolic, Degenerative, and CSF Disorders

Section 6:

Congenital Malformations of the Skull and Brain

This page intentionally left blank

Osborn's Brain

IMAGING, PATHOLOGY, AND ANATOMY

SECOND EDITION

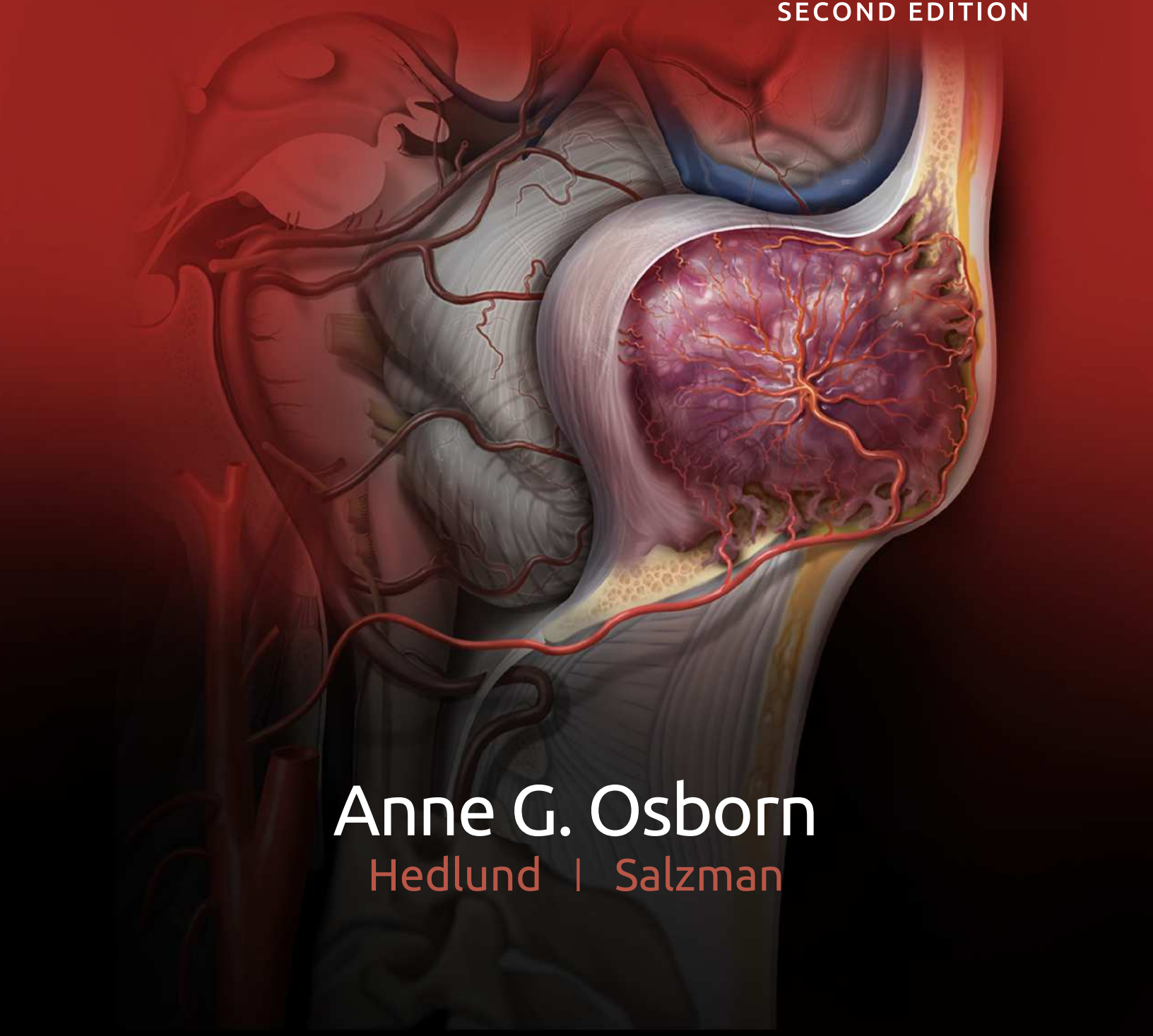

Anne G. Osborn

Hedlund | Salzman

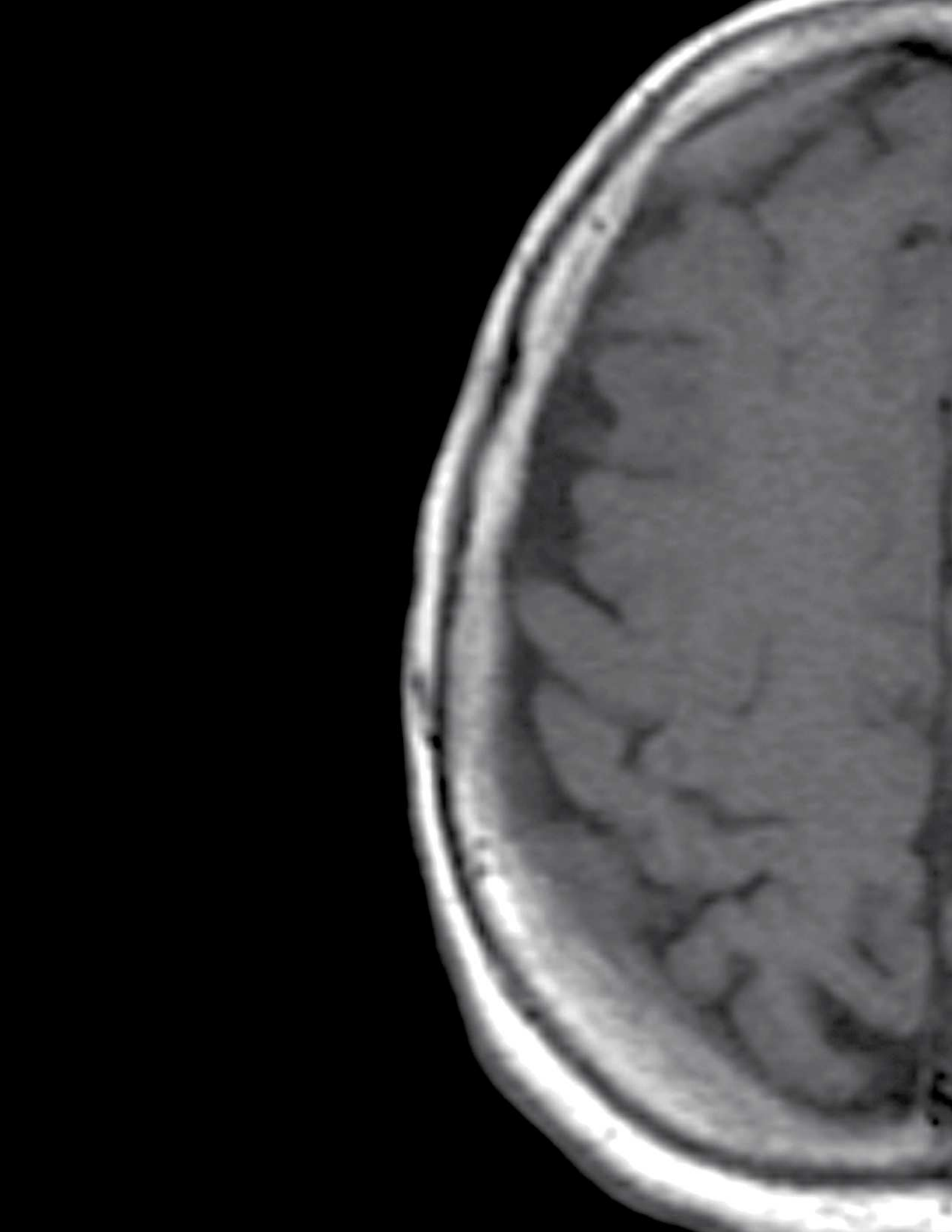

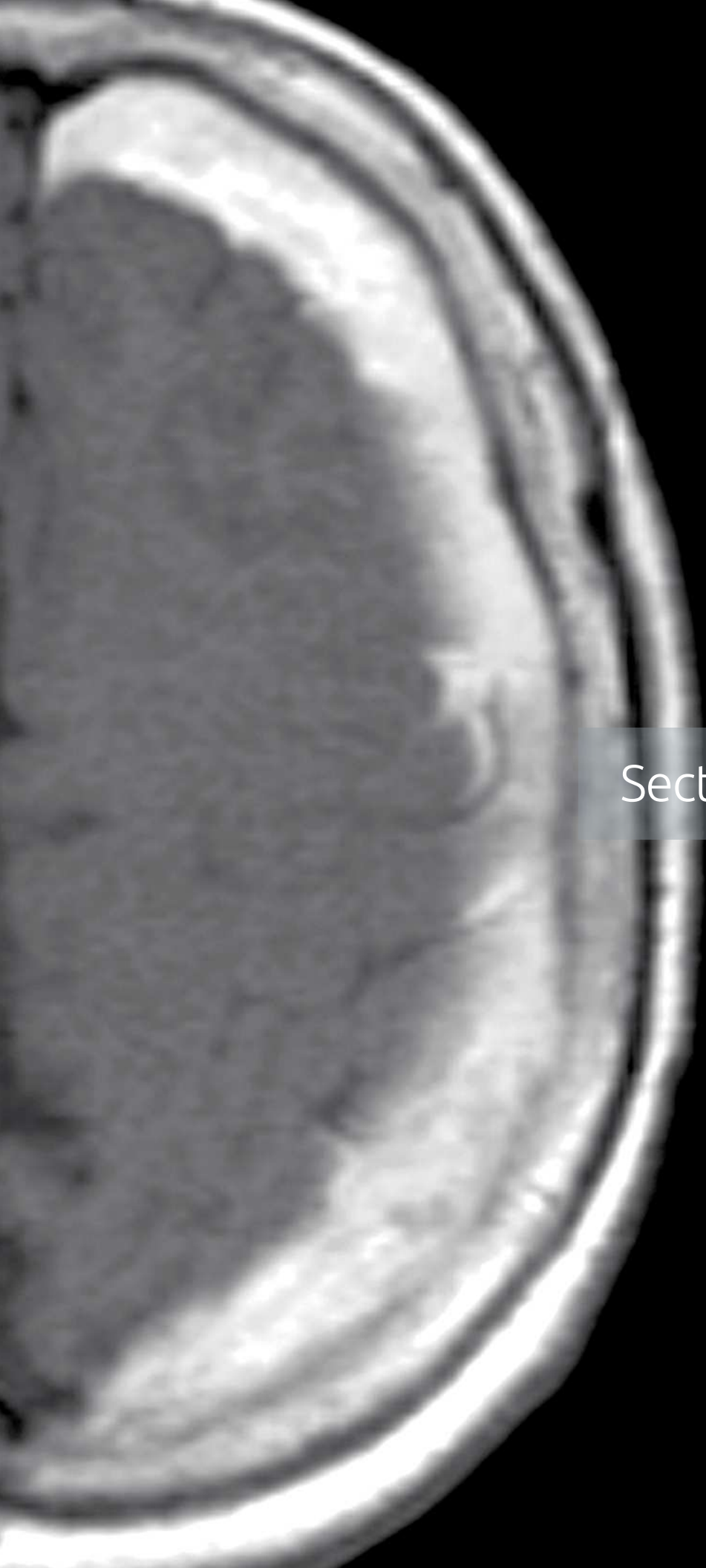

Section 1

Section 1

Trauma

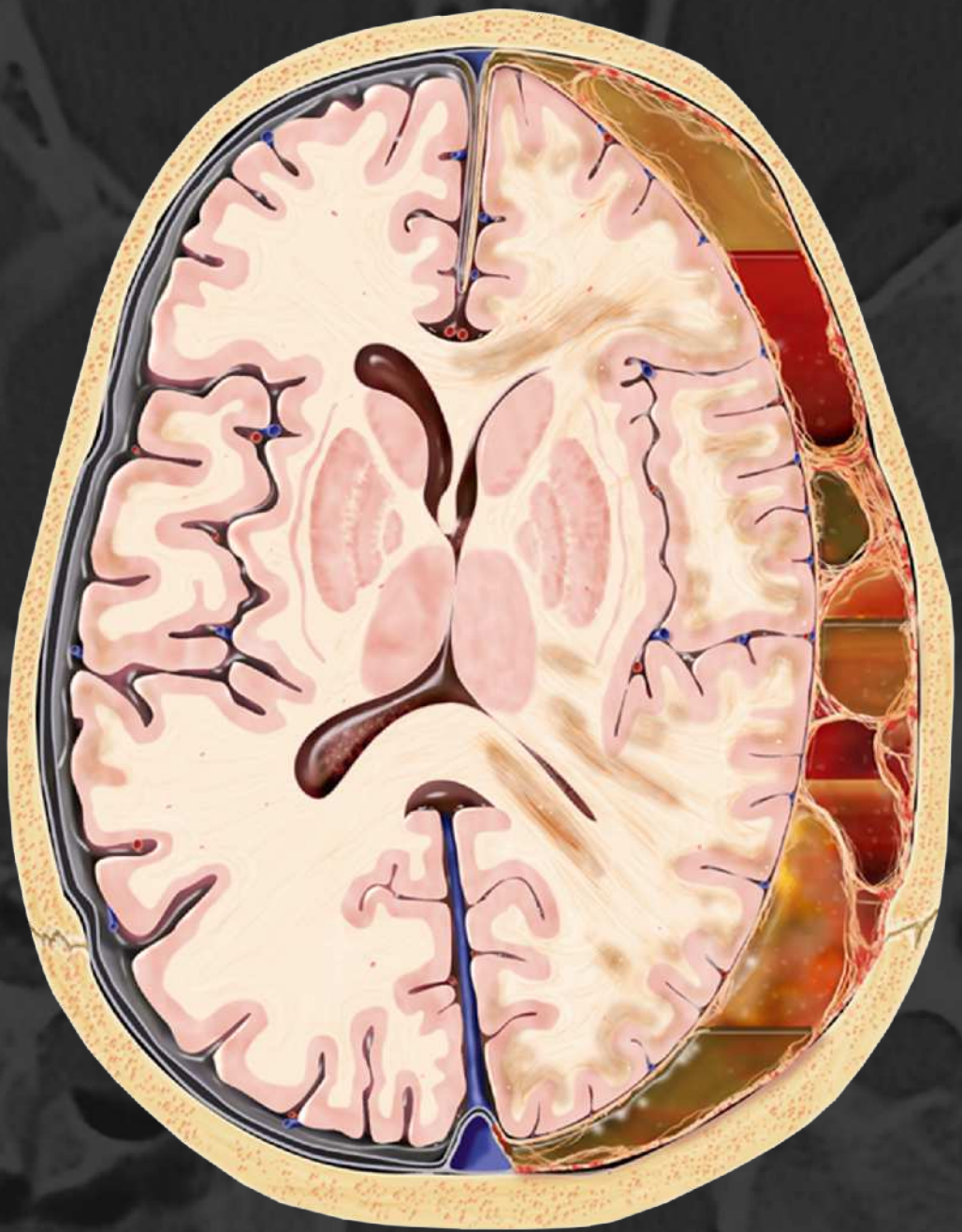

Trauma Overview

Trauma is one of the most frequent indications for emergent neuroimaging. Because imaging plays such a key role in patient triage and management, we begin this book by discussing skull and brain trauma.

We start with a brief consideration of epidemiology. Traumatic brain injury (TBI) is a critical public health and socio-economic problem throughout the world. The direct medical costs of caring for acutely traumatized patients are huge. The indirect costs of lost productivity and long-term care for TBI survivors are even larger than the short-term direct costs.

We then briefly discuss the etiology and mechanisms of head trauma. Understanding the different ways in which the skull and brain can be injured provides the context for understanding the spectrum of findings that can be identified on imaging studies.

Introduction

Epidemiology of Head Trauma

Trauma—sometimes called the "silent epidemic"—is the most common worldwide cause of death in children and young adults. Neurotrauma is responsible for the vast majority of these cases. At least 10 million people worldwide sustain TBI each year. In the USA alone, two million people annually suffer a TBI. Of these, 500,000 require hospital care.

Of all head-injured patients, approximately 10% sustain fatal brain injury. Lifelong disability is common in those who survive. Between 5-10% of TBI survivors have serious permanent neurologic deficits, and an additional 20-40% have moderate disability. Even more have subtle deficits ("minimal brain trauma").

Etiology and Mechanisms of Injury

Trauma can be caused by missile or nonmissile injury. Missile injury results from penetration of the skull, meninges, and/or brain by an external object, such as a bullet. Gunshot wounds are most common in adolescent and young adult male patients but relatively rare in other groups.

Nonmissile closed head injury (CHI) is a much more common cause of neurotrauma than missile injury. Falls have now surpassed road traffic incidents as the leading cause of TBI.

So-called "ground level falls" (GLFs) are a common indication for neuroimaging in young children and older adults. In such cases, brain injury can be significant. With a GLF, a six-foot tall adult's head impacts the ground

at 20 mph. Anticoagulated older adults are especially at risk for intracranial hemorrhages, even with minor head trauma.

Motor vehicle collisions occurring at high speed exert significant acceleration/deceleration forces, causing the brain to move suddenly within the skull. Forcible impaction of the brain against the unyielding calvaria and hard, knife-like dura results in gyral contusion. Rotation and sudden changes in angular momentum may deform, stretch, and damage long vulnerable axons, resulting in axonal injury.

Classification of Head Trauma

The most widely used *clinical* classification of brain trauma, the Glasgow Coma Scale (GCS), depends on the assessment of three features: best eye, verbal, and motor responses. With the use of the GCS, TBI can be designated as a mild, moderate, or severe injury.

TBI can also be divided chronologically and *pathoetiologically* into primary and secondary injury, the system used in this text. **Primary injuries** occur at the time of initial trauma. Skull fractures, epi- and subdural hematomas, contusions, axonal injury, and brain lacerations are examples of primary injuries.

Secondary injuries occur later and include cerebral edema, perfusion alterations, brain herniations, and CSF leaks. Although vascular injury can be immediate (blunt impact) or secondary (vessel laceration from fractures, occlusion secondary to brain herniation), for purposes of discussion, it is included in the chapter on secondary injuries.

CLASSIFICATION OF HEAD TRAUMA

Primary Effects
- Scalp and skull injuries
- Extraaxial hemorrhage/hematomas
- Parenchymal injuries
- Miscellaneous injuries

Secondary Effects
- Herniation syndromes
- Cerebral edema
- Cerebral ischemia
- Vascular injury (can be primary or secondary)

Imaging Acute Head Trauma

Imaging is absolutely critical to the diagnosis and management of the patient with acute TBI. The goal of emergent neuroimaging is twofold: (1) identify treatable injuries, especially emergent ones, and (2) detect and delineate the presence of secondary injuries, such as herniation syndromes and vascular injury.

How To Image?

A broad spectrum of imaging modalities can be used to evaluate patients with TBI. These range from outdated, generally ineffective techniques (e.g., skull radiographs) to very sensitive but expensive studies (e.g., MR). Techniques that are still relatively new include CT and MR perfusion, diffusion tensor imaging (DTI), and functional MRI (fMRI).

Skull Radiography

For decades, skull radiography (whether called "plain film" or, more recently, "digital radiography") was the only noninvasive imaging technique available for the assessment of head injury.

Skull radiography is reasonably effective in identifying calvarial fractures. Yet skull x-rays cannot depict the far more important presence of extraaxial hemorrhages and parenchymal injuries.

Between one-quarter and one-third of autopsied patients with fatal brain injuries have no identifiable skull fracture! Therefore, skull radiography obtained solely for the purpose of identifying the presence of a skull fracture has no appropriate role in the current management of the head-injured patient. With rare exceptions, it's the brain that matters—not the skull!

NECT

Because of its wide availability and rapid detection of acute hemorrhage, CT is now accepted as the worldwide screening tool for imaging acute head trauma. Since its introduction almost 40 years ago, CT has gradually but completely replaced skull radiographs as the "workhorse" of brain trauma imaging. The reasons are simple: CT depicts both bone and soft tissue injuries. It is also widely accessible, fast, effective, and comparatively inexpensive.

Both standard and multidetector row CT (MDCT) are used in the initial imaging of patients with traumatic head injury. Identifying abnormalities that may require urgent treatment to limit secondary injuries, such as brain swelling and herniation syndromes, is essential.

Standard nonenhanced CT (NECT) scans (4 or 5 mm thick) from just below the foramen magnum through the vertex should be performed. Two sets of images should be obtained, one using brain and one with bone reconstruction algorithms. Viewing the brain images with a wider window width (150-200 HU, the so-called subdural window) should be performed on PACS (or film, if PACS is not available). The scout view should always be displayed as part of the study (see below).

MDCT is now in widespread use. Coronal and sagittal reformatted images using the axial source data are routinely performed in head trauma triage and improve the detection rate of acute traumatic subdural hematomas.

Three-dimensional shaded surface displays are helpful in depicting skull and facial fractures. If facial bone CT is also requested, a single MDCT acquisition can be obtained without overlapping radiation exposure to the eye and lower half of the brain.

Head trauma patients with acute intracranial lesions on CT have a higher risk for cervical spine fractures compared with patients with a CT-negative head injury. Because up to one-

third of patients with moderate to severe head injury as determined by the GCS have concomitant spine injury, MDCT of the cervical spine is often obtained together with brain imaging. Soft tissue and bone algorithm reconstructions with multiplanar reformatted images of the cervical spine should be obtained.

As delayed development or enlargement of both extra- and intracranial hemorrhages may occur within 24-36 hours following the initial traumatic event, repeat CT should be obtained if there is sudden unexplained clinical deterioration, regardless of initial imaging findings.

CTA

CT angiography (CTA) is often obtained as part of a whole-body trauma CT protocol. Craniocervical CTA should also specifically be considered (1) in the setting of penetrating neck injury, (2) if a fractured foramen transversarium or facet subluxation is identified on cervical spine CT, or (3) if a skull base fracture traverses the carotid canal or a dural venous sinus. Arterial laceration or dissection, traumatic pseudoaneurysm, carotid-cavernous fistula, or dural venous sinus injury are nicely depicted on high-resolution CTA.

MR

Although MR can detect traumatic complications without radiation and is more sensitive for abnormalities such as contusions and axonal injuries, there is general agreement that NECT is the procedure of choice in the initial evaluation of brain trauma. Limitations of MR include acquisition time, access, patient monitoring and instability, motion degradation of images, and cost.

With one important exception—suspected child abuse—using MR as a routine screening procedure in the setting of *acute* brain trauma is uncommon. Standard MR together with susceptibility-weighted imaging and DTI is most useful in the subacute and chronic stages of TBI. Other modalities such as fMRI are playing an increasingly important role in detecting subtle abnormalities, especially in patients with mild cognitive deficits following minor TBI.

Who and When To Image?

Who to image and when to do it are paradoxically both well established and controversial. Patients with a GCS score indicating moderate (GCS = 9-12) or severe (GCS ≤ 8) neurologic impairment are invariably imaged. The real debate is about how best to manage patients with GCS scores of 13-15.

In an attempt to reduce CT overutilization in emergency departments, several organizations have developed evidence-based clinical criteria that help separate "high-risk" from "low-risk" patients. (Several of these are delineated in the boxes below.) Yet the impact on the emergency department physician ordering behavior has been inconsistent. In places with high malpractice rates, many emergency physicians routinely order NECT scans on every patient with head trauma regardless of GCS score or clinical findings.

Repeat head CT scans in trauma transfers from one hospital to another are common and add to both radiation dose exposure and cost. Inadequate data transfer from the referring hospital—not poor image quality—is the major reason for potentially preventable repeat head CT scans.

Whether—and when—to obtain follow-up imaging in trauma patients is controversial. In a large study of children with GCS scores of 14 or 15 and a normal initial CT scan, only 2% had follow-up CT or MR performed. Of these, only 0.05% had abnormal results on the follow-up study, and *none* required surgical intervention. The negative predictive value for neurosurgical intervention for a child with an initial GCS of 14 or 15 and normal CT was 100%. From this, the authors concluded that children with a GCS of 14 or 15 and a normal initial head CT are at very low risk for subsequent traumatic findings on neuroimaging and extremely low risk of needing neurosurgical intervention. Hospitalization for neurologic observation of children with minor head trauma after normal CT scan results was deemed unnecessary.

GLASGOW COMA SCALE

Best Eye Response (Maximum = 4)
- 1 = no eye opening
- 2 = eye opening to pain
- 3 = eyes open to verbal command
- 4 = eyes open spontaneously

Best Verbal Response (Maximum = 5)
- 1 = none
- 2 = incomprehensible sounds
- 3 = inappropriate words
- 4 = confused
- 5 = oriented

Best Motor Response (Maximum = 6)
- 1 = none
- 2 = extension to pain
- 3 = flexion to pain
- 4 = withdrawal to pain
- 5 = localizing to pain
- 6 = obedience to commands

Sum = "Coma Score" and Clinical Grading
- 13-15 = mild brain injury
- 9-12 = moderate brain injury
- ≤ 8 = severe brain injury

Appropriateness Criteria

Three major and widely used appropriateness criteria for imaging acute head trauma have been published: The American College of Radiology (ACR) Appropriateness Criteria, the New Orleans Criteria (NOC), and the Canadian Head CT Rule (CHCR).

ACR Criteria. Emergent NECT in mild/minor CHI with the presence of a focal neurologic deficit and/or other risk factors is deemed "very appropriate," as is imaging all traumatized children under 2 years of age. Although acknowledging that NECT in patients with mild/minor CHI (GCS ≥ 13) without risk

(1-1A) Axial NECT scan of a prisoner imaged for head trauma shows no gross abnormality. (Courtesy J. A. Junker, MD.)

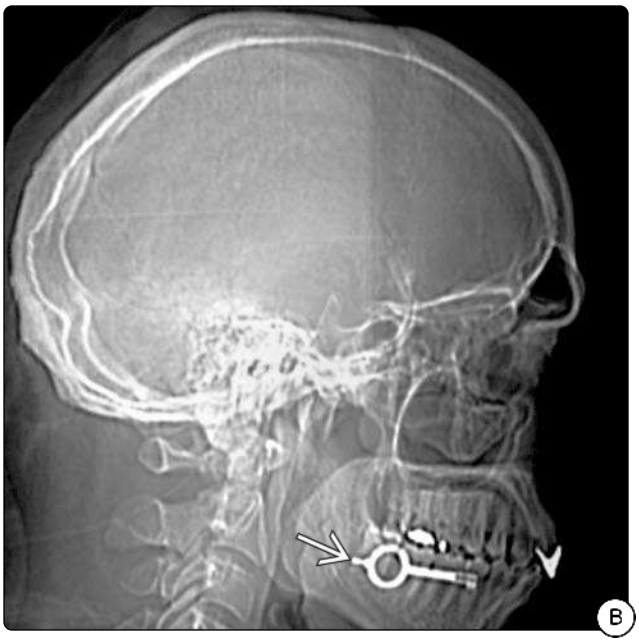

(1-1B) Scout view in the same case shows a foreign object ➔ (a handcuff key!) in the prisoner's mouth. He faked the injury and was planning to escape, but the radiologist alerted the guards and thwarted the plan. (Courtesy J. A. Junker, MD.)

factors or focal neurologic deficit is "known to be low yield," the ACR still rates it as 7 out of 9 in appropriateness.

NOC and CHCR. Both the NOC and CHCR attempt to triage patients with minimal/mild head injuries in a cost-effective manner. A GCS score of 15 (i.e., normal) without any of the NOC indicators is a highly sensitive negative predictor of clinically important brain injury or need for surgical intervention.

NEW ORLEANS CRITERIA IN MINOR HEAD INJURY

CT indicated if GCS = 15 plus any of the following

- Headache
- Vomiting
- Patient > 60 years old
- Intoxication (drugs, alcohol)
- Short-term memory deficits (anterograde amnesia)
- Visible trauma above clavicles
- Seizure

Adapted from Stiell IG et al: Comparison of the Canadian CT head rule and the New Orleans criteria in patients with minor head injury. JAMA 294(12):1511-1518, 2005

According to the CHCR, patients with a GCS score of 13-15 and witnessed loss of consciousness (LOC), amnesia, or confusion are imaged, along with those deemed "high risk" for neurosurgical intervention or "medium risk" for brain injury.

Between 6-7% of patients with minor head injury have positive findings on head CT scans. Most of these patients also have headache, vomiting, drug or alcohol intoxication, seizure, short-term memory deficits, or physical evidence of trauma above the clavicles. CT should be used liberally in these cases, as well as in patients over 65 years of age, children under the age of two, anticoagulated patients, and patients with loss of consciousness or focal neurologic deficit.

Recent studies have also shown that compliance with established imaging guidelines such as the CHCR is poor, particularly in busy EDs that handle large trauma volumes. Despite efforts to educate urgent care physicians about limiting patient exposure to ionizing radiation and using clinically based risk stratification, nonenhanced head CTs remain one of the most frequently overutilized imaging studies.

CANADIAN HEAD CT RULE IN MINOR HEAD INJURY

CT if GCS = 13-15 and witnessed LOC, amnesia, or confusion

High risk for neurosurgical intervention

- GCS < 15 at 2 hours
- Suspected open/depressed skull fracture
- Clinical signs of skull base fracture
- ≥ 2 vomiting episodes
- Age ≥ 65 years

Medium risk for brain injury detected by head CT

- Antegrade amnesia ≥ 30 minutes
- "Dangerous mechanism" (i.e., auto-pedestrian, ejection from vehicle, etc.)

Adapted from Stiell IG et al: Comparison of the Canadian CT head rule and the New Orleans criteria in patients with minor head injury. JAMA 294(12):1511-1518, 2005

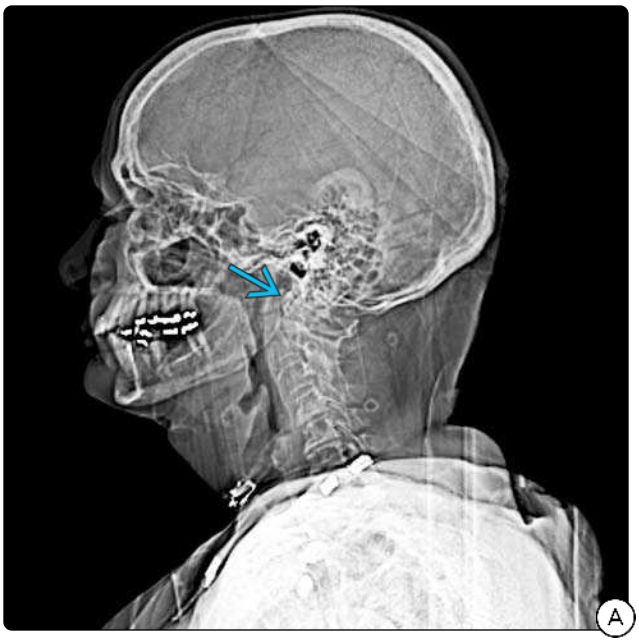

(1-2A) Scout view in a 66y woman with a CT head requested to evaluate ground level fall shows a posteriorly angulated C1-odontoid complex ⇨.

(1-2B) The head CT in the same case (not shown) was normal. Cervical spine CT was then performed. The sagittal image reformatted from the axial scan data shows a comminuted, posteriorly angulated dens fracture ➡.

Trauma Imaging: Keys to Analysis

Four components are essential to the accurate interpretation of CT scans in patients with head injury: the scout image plus brain, bone, and subdural views of the NECT dataset. Critical information may be present on just one of these four components.

Suggestions on how to analyze NECT images in patients with acute head injury are delineated below.

Scout Image

Before you look at the NECT scan, examine the digital scout image! Look for cervical spine abnormalities such as fractures or dislocations, jaw and/or facial trauma, and the presence of foreign objects **(1-1)**. If there is a suggestion of cervical spine fracture or malalignment, MDCT of the cervical spine should be performed before the patient is removed from the scanner **(1-2)**.

Brain Windows

Methodically and meticulously work your way from the outside in. First evaluate the soft tissue images, beginning with the scalp. Look for scalp swelling, which usually indicates the impact point. Carefully examine the periorbital soft tissues.

Next look for extraaxial blood. The most common extraaxial hemorrhage is traumatic subarachnoid hemorrhage (tSAH), followed by sub- and epidural hematomas. The prevalence of tSAH in moderate to severe TBI approaches 100%. tSAH is usually found in the sulci adjacent to cortical contusions, along the sylvian fissures, and around the anteroinferior frontal and temporal lobes. The best place to look for subtle tSAH is the interpeduncular cistern, where blood collects when the patient is supine.

Any hypodensity within an extraaxial collection should raise suspicion of rapid hemorrhage with accumulation of unclotted blood or (especially in alcoholics or older patients) an underlying coagulopathy. This is an urgent finding that mandates immediate notification of the responsible clinician.

Look for intracranial air ("pneumocephalus"). Intracranial air is always abnormal and indicates the presence of a fracture that traverses either the paranasal sinuses or mastoid.

Now move on to the brain itself. Carefully examine the cortex, especially the "high-yield" areas for cortical contusions (anteroinferior frontal and temporal lobes). If there is a scalp hematoma due to impact (a "coup" injury), look 180° in the opposite direction for a classic "contre-coup" injury. Hypodense areas around the hyperdense hemorrhagic foci indicate early edema and severe contusion.

Move inward from the cortex to the subcortical white and deep gray matter. Petechial hemorrhages often accompany axonal injury. If you see subcortical hemorrhages on the initial NECT scan, this is merely the "tip of the iceberg." There is usually *a lot* more damage than what is apparent on the first scan. A general rule: the deeper the lesion, the more severe the injury.

Finally, look inside the ventricles for blood-CSF levels and hemorrhage due to choroid plexus shearing injury.

Subdural Windows

Look at the soft tissue image with both narrow ("brain") and intermediate ("subdural") windows. Small subtle subdural hematomas can sometimes be overlooked on standard narrow window widths (75-100 HU) yet are readily apparent when wider windows (150-200 HU) are used.

Bone CT

Bone CT refers to bone algorithm reconstruction viewed with wide (bone) windows. If you can't do bone algorithm reconstruction from your dataset, widen the windows and use an edge-enhancement feature to sharpen the image. Three-dimensional shaded surface displays (3D SSDs) are especially helpful in depicting complex or subtle fractures **(1-3)**.

Even though standard head scans are 4-5 mm thick, it is often possible to detect fractures on bone CT. Look for basisphenoid fractures with involvement of the carotid canal, temporal bone fractures (with or without ossicular dislocation), mandibular dislocation ("empty" condylar fossa), and calvarial fractures. And remember: nondisplaced linear skull fractures that don't cross vascular structures (such as a dural venous sinus or middle meningeal artery) are in and of themselves basically meaningless. The brain and blood vessels are what matter!

The most difficult dilemma is deciding whether an observed lucency is a fracture or a normal structure (e.g., suture line or vascular channel). Keep in mind: it is virtually unheard of for a calvarial fracture to occur in the absence of overlying soft tissue injury. If there is no scalp "bump," it is unlikely that the lucency represents a nondisplaced linear fracture.

Bone CT images are also very helpful in distinguishing low density from air vs. fat. Although most PACS stations have a region of interest (ROI) function that can measure attenuation, fat fades away on bone CT images, and air remains very hypodense.

(1-3A) Axial NECT in an 18y man who fell off his skateboard shows a small right epidural hematoma that also contains air ⇒. (1-3B) Two-millimeter bone algorithm reconstruction in the same case shows a nondisplaced linear fracture of the squamous temporal bone ⇒ adjacent to the epidural blood and air ⇒.

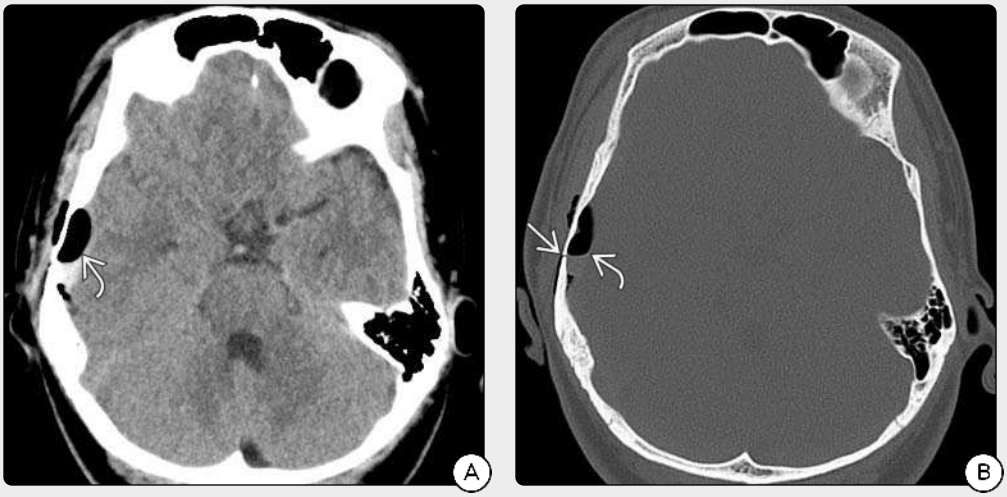

(1-3C) Coronal (left) and sagittal (right) bone CTs reconstructed from the axial source data show the temporal bone fracture ⇒ is comminuted and crosses the mastoid ⇒ and middle ear ⇒. (1-3D) Bone CT with shaded surface display in the same case nicely shows the squamous ⇒, mastoid ⇒ aspects of the nondisplaced but comminuted fracture.

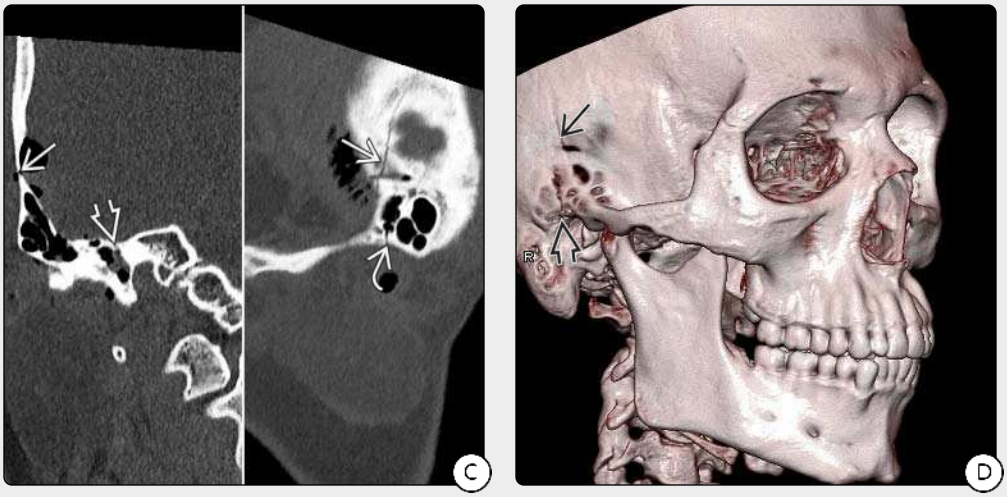

CTA

CTA is generally indicated if (1) basilar skull fractures cross the carotid canal or a dural venous sinus **(1-4)**; (2) if a cervical spine fracture-dislocation is present, especially if the transverse foramina are involved; or (3) if the patient has stroke-like symptoms or unexplained clinical deterioration. Both the cervical and intracranial vasculature should be visualized.

Although it is important to scrutinize both the arterial and venous sides of the circulation, a CTA is generally sufficient. Standard CTAs typically show both the arteries and the dural venous sinuses well, whereas a CT venogram (CTV) often misses the arterial phase.

Examine the source images as well as the multiplanar reconstructions and maximum-intensity projection (MIP) reformatted scans. Traumatic dissection, vessel lacerations, intimal flaps, pseudoaneurysms, carotid-cavernous fistulas, and dural sinus occlusions can generally be identified on CTA.

HEAD TRAUMA: CT CHECKLIST

Scout Image
- Evaluate for
  - Cervical spine fracture-dislocation
  - Jaw dislocation, facial fractures
  - Foreign object

Brain Windows
- Scalp swelling (impact point)
- Extraaxial blood (focal hypodensity in clot suggests rapid bleeding)
  - Epidural hematoma
  - Subdural hematoma (SDH)
  - Traumatic subarachnoid hemorrhage
- Pneumocephalus
- Cortical contusion
  - Anteroinferior frontal, temporal lobes
  - Opposite scalp laceration/skull fracture
- Hemorrhagic axonal injury
- Intraventricular hemorrhage

Subdural Windows
- 150-200 HU (for thin SDHs under skull)

Bone CT
- Bone algorithm reconstruction > bone windows
- Any fractures cross a vascular channel?

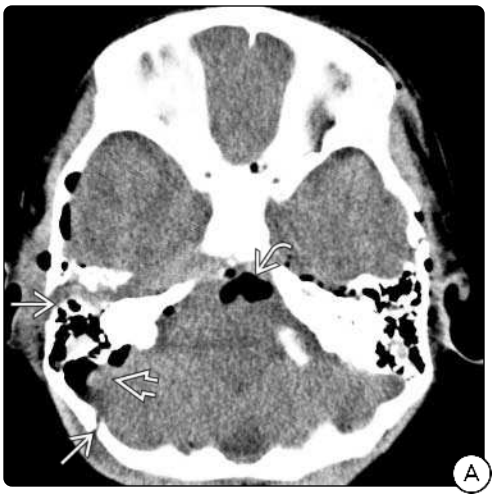

(1-4A) NECT shows pneumocephalus, base of skull fractures adjacent to air, which seems to outline a displaced sigmoid sinus.

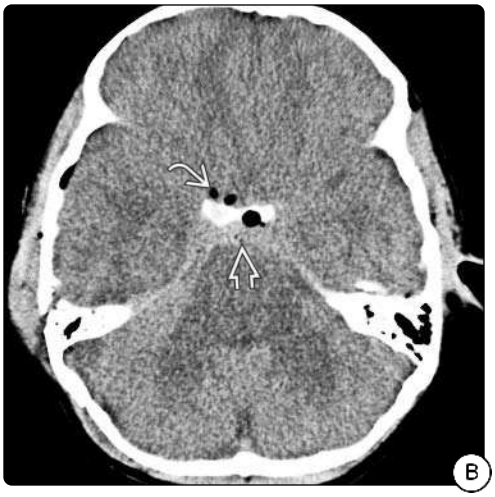

(1-4B) NECT in the same case shows diffuse brain swelling, pneumocephalus, and traumatic subarachnoid hemorrhage.

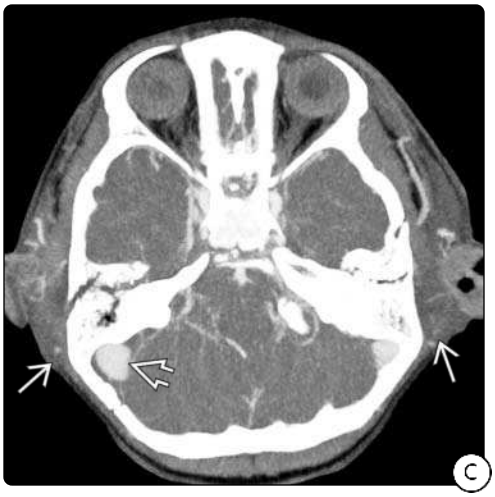

(1-4C) CTA in the same case shows the sigmoid sinus is intact but displaced medially. Note rapidly enlarging subgaleal hematoma.

Selected References

Introduction

Epidemiology of Head Trauma

Roozenbeek B et al: Changing patterns in the epidemiology of traumatic brain injury. Nat Rev Neurol. 9(4):231-6, 2013

Imaging Acute Head Trauma

How To Image?

Amrhein TJ et al: Reformatted images improve the detection rate of acute traumatic subdural hematomas on brain CT compared with axial images alone. Emerg Radiol. 24(1):39-45, 2017

Hinzpeter R et al: Repeated CT scans in trauma transfers: an analysis of indications, radiation dose exposure, and costs. Eur J Radiol. 88:135-140, 2017

Raja AS et al: "Choosing wisely" imaging recommendations: initial implementation in New England emergency departments. West J Emerg Med. 18(3):454-458, 2017

Thesleff T et al: Head injuries and the risk of concurrent cervical spine fractures. Acta Neurochir (Wien). 159(5):907-914, 2017

Lolli V et al: MDCT imaging of traumatic brain injury. Br J Radiol. 20150849, 2016

Bodanapally UK et al: Imaging of traumatic brain injury. Radiol Clin North Am. 53(4):695-715, viii, 2015

Who and When To Image?

Granata RT et al: Safety of deferred CT imaging of intoxicated patients presenting with possible traumatic brain injury. Am J Emerg Med. 35(1):51-54, 2017

Sharp AL et al: Computed tomography use for adults with head injury: describing likely avoidable emergency department imaging based on the Canadian CT head rule. Acad Emerg Med. 24(1):22-30, 2017

Atabaki SM et al: Comparison of prediction rules and clinician suspicion for identifying children with clinically important brain injuries after blunt head trauma. Acad Emerg Med. 23(5):566-75, 2016

Bharadwaj S et al: Minor head injury: limiting patient exposure to ionizing radiation, risk stratification, and concussion management. Curr Opin Pediatr. 28(1):121-31, 2016

Lolli V et al: MDCT imaging of traumatic brain injury. Br J Radiol. 20150849, 2016

Sadegh R et al: Head CT scan in Iranian minor head injury patients: evaluating current decision rules. Emerg Radiol. 23(1):9-16, 2016

Arab AF et al: Accuracy of Canadian CT head rule in predicting positive findings on CT of the head of patients after mild head injury in a large trauma centre in Saudi Arabia. Neuroradiol J. 28(6):591-7, 2015

Bodanapally UK et al: Imaging of traumatic brain injury. Radiol Clin North Am. 53(4):695-715, viii, 2015

Gunes Tatar I et al: Appropriateness of selection criteria for CT examinations performed at an emergency department. Emerg Radiol. 21(6):583-8, 2014

Ryan ME et al: ACR appropriateness criteria head trauma--child. J Am Coll Radiol. 11(10):939-47, 2014

Stiell IG et al: Comparison of the Canadian CT Head Rule and the New Orleans Criteria in patients with minor head injury. JAMA. 294(12):1511-8, 2005

Primary Effects of CNS Trauma

Primary head injuries are defined as those that occur at the time of initial trauma even though they may not be immediately apparent on initial evaluation.

Head injury can be caused by direct or indirect trauma. **Direct trauma** involves a blow to the head and is usually caused by automobile collisions, falls, or injury inflicted by an object such as a hammer or baseball bat. Scalp lacerations, hematomas, and skull fractures are common. Associated intracranial damage ranges from none to severe.

Significant forces of acceleration/deceleration, linear translation, and rotational loading can be applied to the brain *without* direct head blows. Such **indirect trauma** is caused by angular kinematics and typically occurs in high-speed motor vehicle collisions (MVCs). Here the brain undergoes rapid deformation and distortion. Depending on the site and direction of the force applied, significant injury to the cortex, axons, penetrating blood vessels, and deep gray nuclei may occur. Severe brain injury can occur in the absence of skull fractures or visible scalp lesions.

We begin our discussion with a consideration of scalp and skull lesions as we work our way from the outside to the inside of the skull. We then delineate the spectrum of intracranial trauma, starting with extraaxial hemorrhages. We conclude this chapter with a detailed discussion of injuries to the brain parenchyma (e.g., cortical contusion, diffuse axonal injury, and the serious deep subcortical injuries).

Scalp and Skull Injuries

Scalp and skull injuries are common manifestations of cranial trauma. Although brain injury is usually the most immediate concern in managing traumatized patients, superficial lesions such as scalp swelling and focal hematoma can be helpful in identifying the location of direct head trauma. On occasion, these initially innocent-appearing "lumps and bumps" can become life-threatening. Before turning our attention to intracranial traumatic lesions, we therefore briefly review scalp and skull injuries, delineating their typical imaging findings and clinical significance.

Scalp Injuries

Scalp injuries include lacerations and hematomas. Scalp **lacerations** can occur in both penetrating and closed head injuries. Lacerations may extend partially or entirely through all five layers of the scalp (skin, subcutaneous fibrofatty tissue, galea aponeurotica, loose areolar connective tissue, and periosteum) to the skull **(2-1)**.

Focal discontinuity, soft tissue swelling, and subcutaneous air are commonly identified in scalp lacerations. Scalp lacerations should be carefully evaluated

***(2-1)** Coronal graphic depicts normal layers of the scalp. Skin, subcutaneous fibrofatty tissue overlie the galea aponeurotica ⇨, loose areolar connective tissue. The pericranium ⇨ is the periosteum of the skull and continues into and through sutures to merge with the periosteal layer of the dura ⇨. **(2-2)** NECT shows scalp laceration ⇨, hyperdense foreign bodies ⇨, and subgaleal air ⇨.*

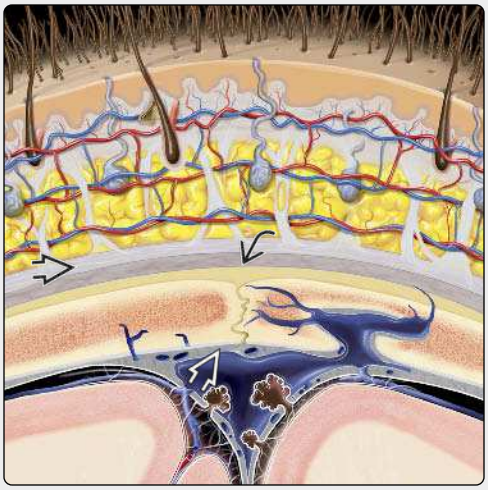

***(2-3)** Graphic shows the skull of a newborn, including the anterior fontanelle, coronal, metopic, sagittal sutures. Cephalohematoma ⇨ is subperiosteal, limited by sutures. Subgaleal hematoma ⇨ is under the scalp aponeurosis, not bounded by sutures. **(2-4A)** NECT scan in a newborn shows a small right ⇨ and a large left ⇨ parietal cephalohematoma. Neither crosses the sagittal suture ⇨.*

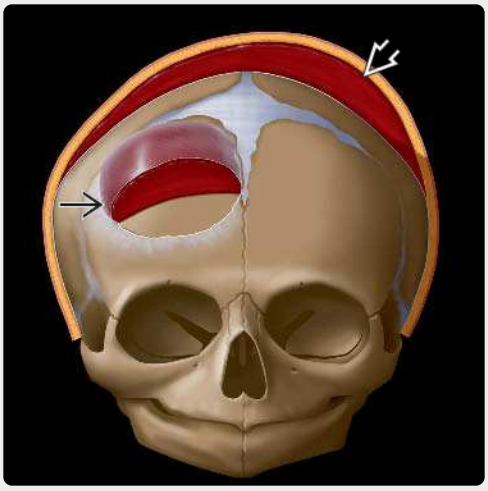

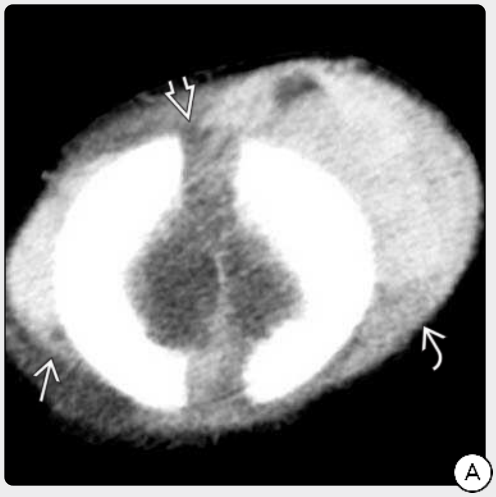

***(2-4B)** Coronal scan in the same case shows the small right ⇨, large left-sided cephalohematomas ⇨. The elevated periosteum ⇨ clearly separates the two blood collections. **(2-4C)** Sagittal scan reformatted from the axial data shows that the left parietal cephalohematoma ⇨ does not cross the coronal suture ⇨.*

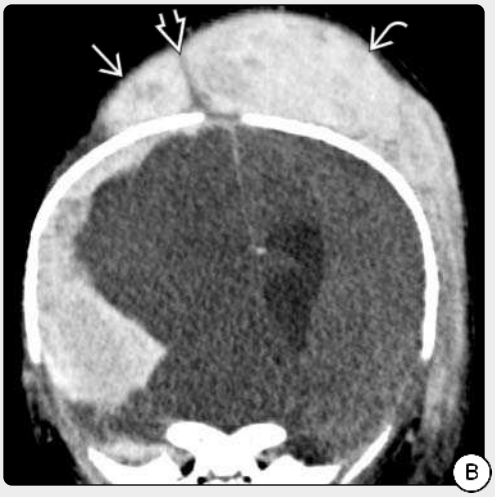

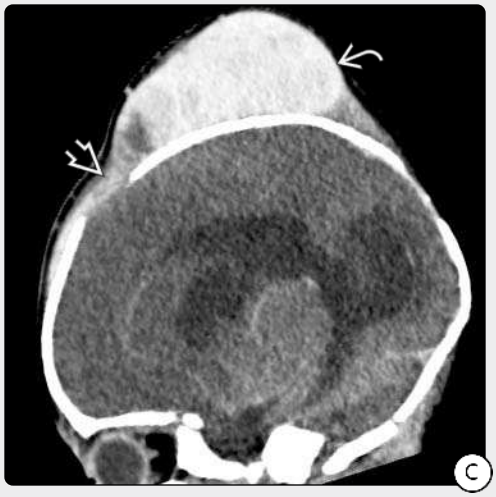

for the presence of any foreign bodies. If not removed during wound debridement, foreign bodies can be a potential source of substantial morbidity and are very important to identify on initial imaging studies. Wood fragments are often hypodense, whereas leaded glass, gravel, and metallic shards are variably hyperdense **(2-2)**.

Scalp lacerations may or may not be associated with scalp **hematomas**. There are two distinctly different types of scalp hematomas: cephalohematomas and subgaleal hematomas. The former are usually of no clinical significance, whereas the latter can cause hypovolemia and hypotension.

Cephalohematomas are *subperiosteal* blood collections that lie in the potential space between the outer surface of the calvarium and the pericranium, which serves as the periosteum of the skull **(2-3)**. The pericranium continues medially into cranial sutures and is anatomically contiguous with the outer (periosteal) layer of the dura.

Cephalohematomas are the extracranial equivalent of an intracranial epidural hematoma. Cephalohematomas do not cross suture lines and are typically unilateral. Because they are anatomically constrained by the tough fibrous periosteum and its insertions, cephalohematomas rarely attain large size.

Cephalohematomas occur in 1% of newborns and are more common following instrumented delivery. They are often diagnosed clinically but imaged only if they are unusually prominent or if intracranial injuries are suspected. NECT scans show a somewhat lens-shaped soft tissue mass that overlies a single bone (usually the parietal or occipital bone) **(2-4)**. If more than one bone is affected, the two collections are separated by the intervening suture lines.

Complications from cephalohematoma are rare, and most resolve spontaneously over a few days or weeks. Occasionally the elevated periosteum at the periphery of a chronic cephalohematoma undergoes dystrophic calcification, creating a firm palpable mass.

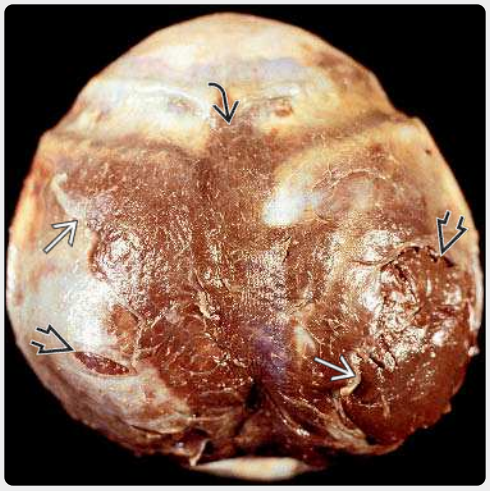

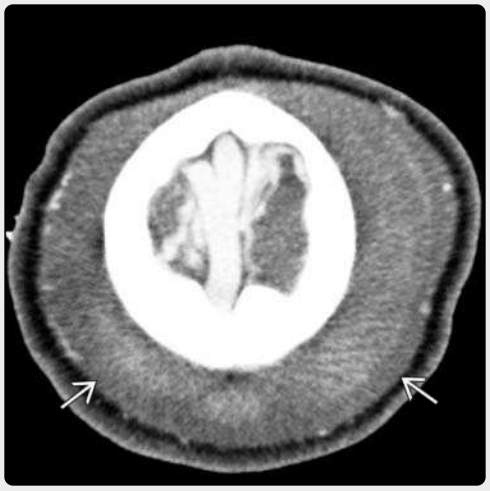

(2-5) Autopsy from a traumatized infant shows a massive biparietal subgaleal hematoma ➡. The galea aponeurotica has been partially opened ⇨ to show large biparietal hematoma that crosses the sagittal suture ⇨. (2-6) Axial CECT in 3y child shows massive subgaleal hematoma ➡ surrounding entire calvarium. Subgaleal hematomas cross sutures, can become life-threatening, while cephalohematomas are anatomically limited.

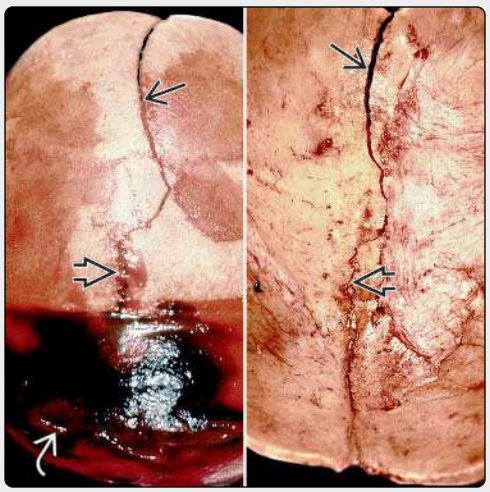

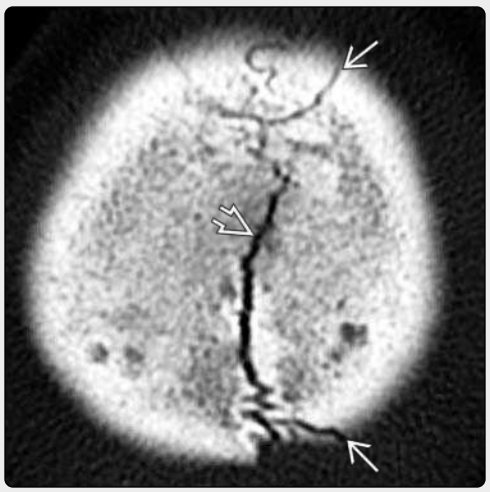

(2-7) Autopsied skull shows fatal trauma with exo- (L) and endocranial views (R). A linear fracture ⇨ extends into the superior sagittal suture ⇨, causing diastasis and a subgaleal hematoma ➡. (2-8) Bone CT through the top of the calvarium shows linear skull fractures ➡ extending into and widening the sagittal suture, causing a diastatic fracture ➡.

Subgaleal hematomas are *subaponeurotic* collections and are common findings in traumatized patients of all ages. Here blood collects under the aponeurosis (the "galea") of the occipitofrontalis muscle **(2-5)**. Because a subgaleal hematoma lies deep to the scalp muscles and galea aponeurotica but external to the periosteum, it is not anatomically limited by suture lines.

Bleeding into the subgaleal space can be very extensive. Subgaleal hematomas are usually bilateral lesions that often spread diffusely around the entire calvaria. NECT scans show a heterogeneously hyperdense crescentic scalp mass that crosses one or more suture lines **(2-6)**.

Most subgaleal hematomas resolve without treatment. In contrast to benign self-limited cephalohematomas, however, expanding subgaleal hematomas in infants and small children can cause significant blood loss.

Facial Injuries

Facial fractures are commonly overlooked on initial imaging (typically head CT scans). Important soft tissue markers can be identified that correlate with facial fractures and may merit a dedicated CT evaluation of the facial bones. These include periorbital contusions and subconjunctival hemorrhage as well as lacerations of the lips, mouth, and nose.

Holmgren et al. (2005) have proposed the mnemonic LIPS-N (**l**ip laceration, **i**ntraoral laceration, **p**eriorbital contusion, **s**ubconjunctival hemorrhage, and **n**asal laceration) be used in conjunction with physical examination. If any of these is present, a traumatized patient should have a dedicated facial CT in addition to the standard head CT.

Skull Fractures

Noticing a scalp "bump" or hematoma on initial imaging in head trauma is important, as calvarial fractures rarely—if

***(2-9)** 3D shaded surface display (SSD) in a patient with multiple linear ⇨ and diastatic ⇨ skull fractures shows utility of SSDs in depicting complex fracture anatomy. Note slight depression ⇨ of the fractured parieto-occipital calvarium. **(2-10A)** Axial bone CT in a patient who was hit in the head with a falling ladder shows an extensively comminuted, depressed skull fracture ⇨.*

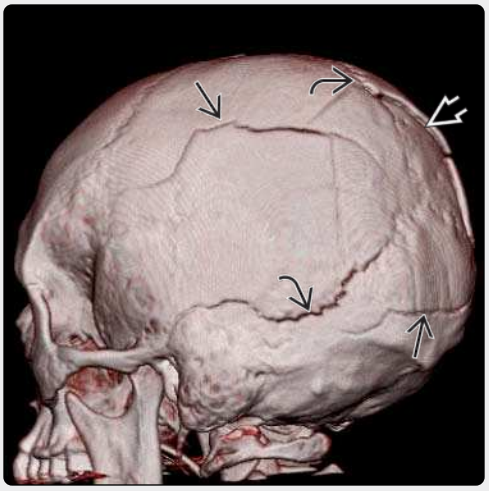

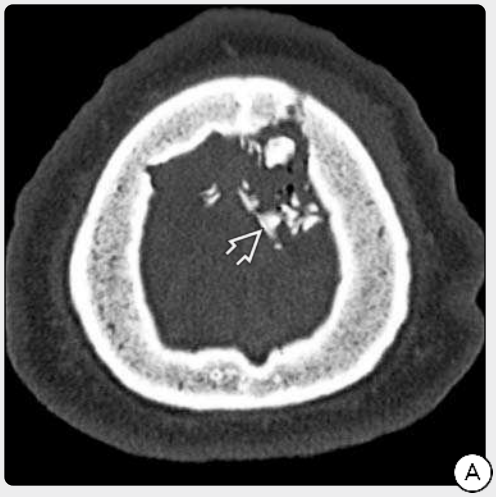

***(2-10B)** Coronal bone CT reformatted from the axial source data in the same case shows that the depressed skull fracture ⇨ is near the midline, raising concern for superior sagittal sinus injury. **(2-10C)** Sagittal bone CT in the same case shows the depressed skull fracture ⇨, associated with a focal scalp hematoma ⇨. CTV (not shown) demonstrated SSS narrowing without occlusion or venous EDH.*

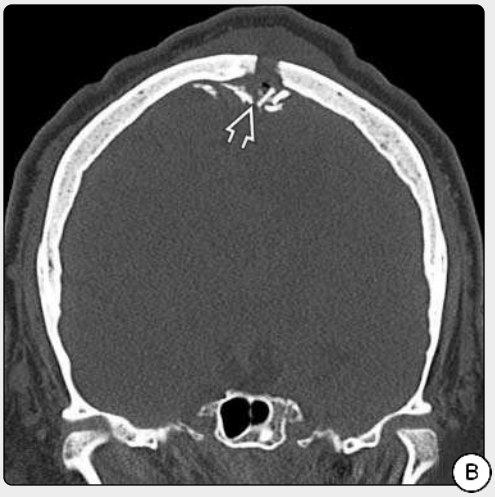

ever—occur in the absence of overlying soft tissue swelling or scalp laceration. Skull fractures are present on initial CT scans in about two-thirds of patients with moderate head injury, although 25-35% of severely injured patients have no identifiable fracture even with thin-section bone reconstructions.

Skull fractures can be simple or comminuted, closed or open. In open fractures, skin laceration results in communication between the external environment and intracranial cavity. Infection risk is high in this type of fracture, as it is with fractures that cross the mastoids and paranasal sinuses.

Several types of acute skull fracture can be identified on imaging studies: linear, depressed, elevated, and diastatic fractures **(2-7)**. Fractures can involve the calvaria, skull base, or both. Another type of skull fracture, a "growing" skull fracture, is a rare but important complication of skull trauma.

Linear Skull Fractures

A **linear skull fracture** is a sharply marginated linear defect that typically involves both the inner and outer tables of the calvaria **(2-8)**.

Most linear skull fractures are caused by relatively low-energy blunt trauma that is delivered over a relatively wide surface area. Linear skull fractures that extend into and widen a suture become diastatic fractures (see below). When multiple complex fractures are present, 3D shaded surface display (SSD) can be very helpful in depicting their anatomy and relationships to cranial sutures.

Patients with an isolated linear nondisplaced skull fracture (NDSF), no intracranial hemorrhage or pneumocephalus, normal neurologic examination, and absence of other injuries are at very low risk for delayed hemorrhage or other life-threatening complication. Hospitalization is not necessary for many children with NDSFs.

***(2-11A)** Axial NECT scan shows severe scalp laceration ⇨ with a combination of elevated ⇨, depressed ⇨ skull fractures. **(2-11B)** Bone CT in the same case shows that the elevated fracture is literally "hinged" away from the calvaria.*

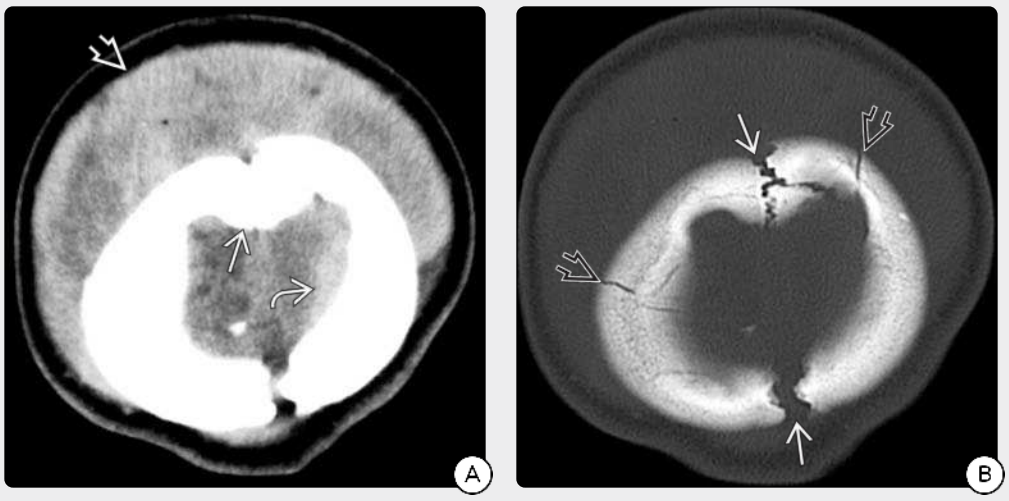

***(2-12A)** Axial NECT scan in a 20y man who had a tree fall on his head shows a massive subgaleal hematoma ⇨ crossing the anterior aspect of the sagittal suture ⇨. A small extraaxial hematoma ⇨, most likely a venous epidural hematoma, is present. **(2-12B)** Bone CT in the same case shows a diastatic fracture of the sagittal suture ⇨. Nondisplaced linear fractures ⇨ are also present.*

Depressed Skull Fractures

A **depressed skull fracture** is a fracture in which the fragments are displaced inward **(2-9)**. Comminution of the fracture fragments starts at the point of maximum impact and spreads centrifugally. Depressed fractures are most often caused by high-energy direct blows to a small surface with a blunt object (e.g., hammer, baseball bat, or metal pipe) **(2-10)**.

Depressed skull fractures typically tear the underlying dura and arachnoid and are associated with cortical contusions and potential leakage of CSF into the subdural space. Fractures extending to a dural sinus or the jugular bulb are associated with venous sinus thrombosis in 40% of cases.

Elevated Skull Fractures

An **elevated skull fracture**—often combined with depressed fragments—is uncommon. Elevated fractures are usually caused by a long, sharp object (such as a machete or propeller) that fractures the calvaria, simultaneously lifting and rotating the fracture fragment **(2-11)**.

Diastatic Skull Fractures

A **diastatic skull fracture** is a fracture that widens ("diastases" or "splits open") a suture or synchondrosis. Diastatic skull fractures usually occur in association with a linear skull fracture that extends into an adjacent suture **(2-12)**.

Traumatic diastasis of the sphenooccipital, petrooccipital, and/or occipitomastoid synchondroses is common in children with severely comminuted central skull base fractures. As it typically does not ossify completely until the mid teens, the sphenooccipital synchondrosis is the most common site.

"Growing" Skull Fractures

A **"growing" skull fracture** (GSF), also known as "posttraumatic leptomeningeal cyst" or "craniocerebral

***(2-13A)** Axial NECT scan in a patient with progressive right hemiparesis following prior head trauma shows left parietal encephalomalacia ➡. The overlying skull appears focally deformed and thinned ⇨. **(2-13B)** Bone CT in the same patient shows a wide lucent skull lesion with rounded, scalloped margins ⇨.*

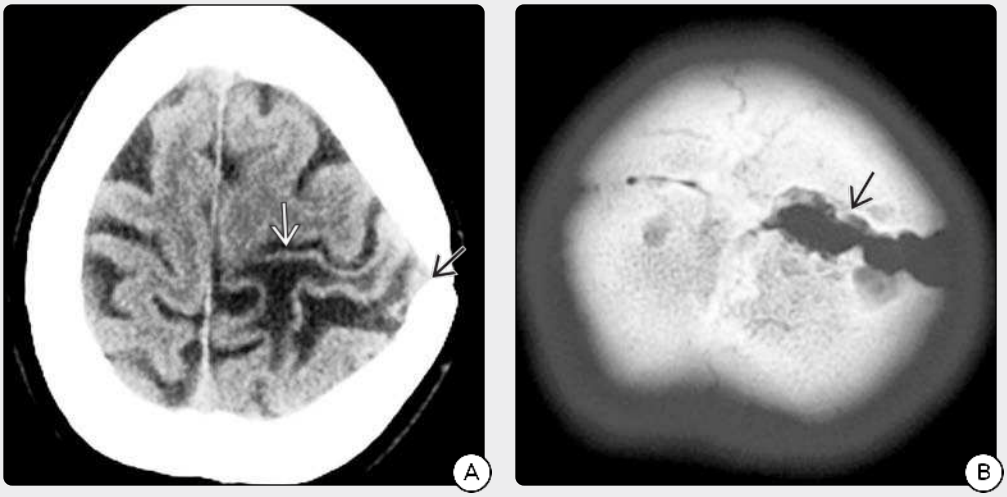

***(2-13C)** Axial T2WI in the same patient shows a lobulated CSF collection ➡ that extends into and almost completely through the calvarial vault. **(2-13D)** Coronal T2WI shows the intradiploic CSF collection ➡ with encephalomalacic brain stretched and tethered into the lesion ⇨. This is classic "growing" skull fracture (leptomeningeal cyst).*

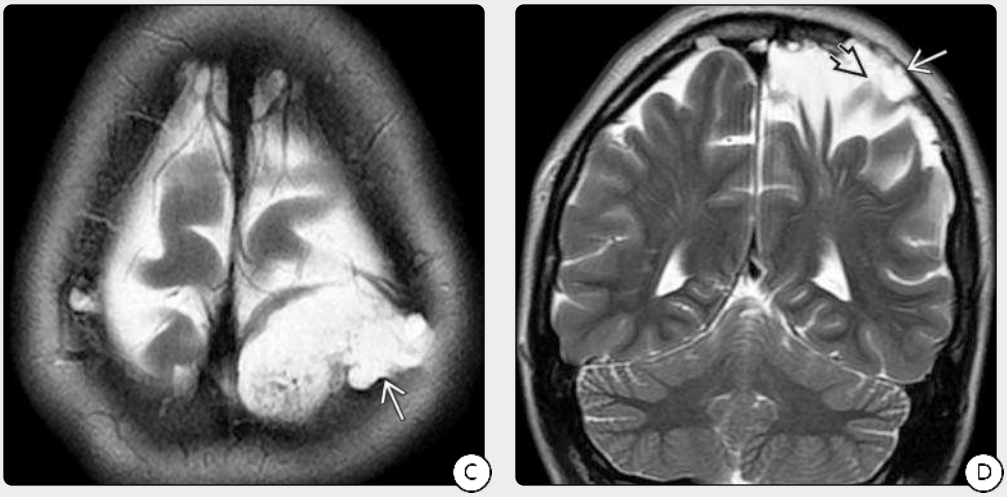

erosion," is a rare lesion that occurs in just 0.3-0.5% of all skull fractures **(2-13)**. Most patients with GSF are under 3 years of age.

GSFs develop in stages and slowly widen over time. In the first "prephase," a skull fracture (typically a linear or comminuted fracture) lacerates the dura, and brain tissue or arachnoid membrane herniates through the torn dura. Stage I extends from the time of initial injury to just before the fracture enlarges. Early recognition and dural repair of stage I GSFs produce the best results.

Stage II is the early phase of GSF. Stage II lasts for approximately 2 months following initial fracture enlargement. At this stage, the bone defect is small, the skull deformity is relatively limited, and neurologic deficits are mild. Nevertheless, the entrapped tissue prevents normal fracture healing.

Stage III represents late-stage GSF and begins 2 months after the initial enlargement begins. During this stage, the bone defect becomes significantly larger. Brain tissue and CSF extend between the bony edges of the fracture through torn dura and arachnoid.

Patients with late-stage GSFs often present months or even years after head trauma. Stage III GSFs can cause pronounced skull deformities and progressive neurologic deficits if left untreated.

Imaging

General Features. Plain skull radiographs have no role in the modern evaluation of traumatic head injury. One-quarter of patients with fatal brain injuries have no skull fracture at autopsy. CT is fast, widely available, sensitive for both bone and brain injury, and the worldwide diagnostic standard of care for patients with head injuries. New generations of multislice CT scanners offer very short acquisition times with excellent spatial resolution.

Both bone and soft tissue reconstruction algorithms should be used when evaluating patients with head injuries. Soft tissue reconstructions should be viewed with both narrow ("brain") and intermediate ("subdural") windows. Coronal and sagittal reformatted images obtained using the axial source data are helpful additions.

Three-dimensional reconstruction and curved MIPs of the skull have been shown to improve fracture detection over the use of axial sections alone.

CT Findings. While fractures can involve any part of the calvaria or skull base, the middle cranial fossa is most susceptible because of its thin "squamous" bones and multiple foramina and fissures.

NECT scans demonstrate *linear* skull fractures as sharply marginated lucent lines. *Depressed* fractures are typically comminuted and show inward implosion of fracture fragments **(2-10)**. *Elevated* fractures show an elevated, rotated skull segment **(2-11)**. Diastatic fractures appear as widened sutures or synchondroses **(2-14)** **(2-15)** and are usually associated with linear skull fractures.

Stage I "*growing*" fractures are difficult to detect on initial NECT scans, as scalp and contused brain are similar in density. Identifying torn dura with herniated brain tissue is similarly difficult although cranial ultrasound can be more helpful.

Later-stage GSFs demonstrate a progressively widening and unhealing fracture. A lucent skull lesion with rounded, scalloped margins and beveled edges is typical **(2-13)**. CSF and soft tissue are entrapped within the expanding fracture. Most GSFs are directly adjacent to posttraumatic encephalomalacia, so the underlying brain often appears hypodense.

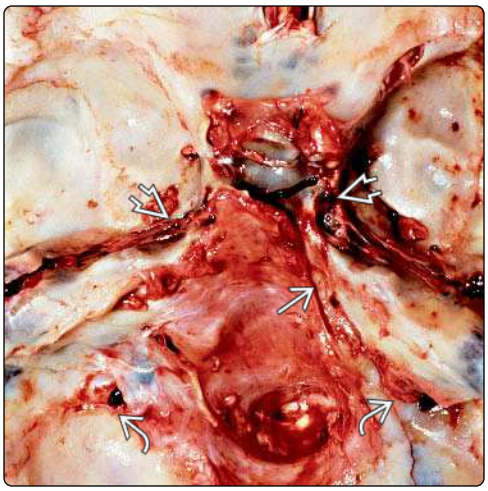

(2-14) Autopsy shows multiple skull base fractures involving clivus, carotid canals, jugular foramina. (E. T. Hedley-White, MD.)

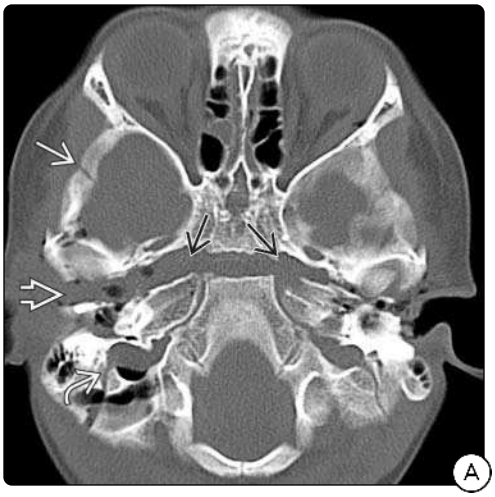

(2-15A) Linear, diastatic fractures of the skull base are present crossing the jugular foramen, both carotid canals.

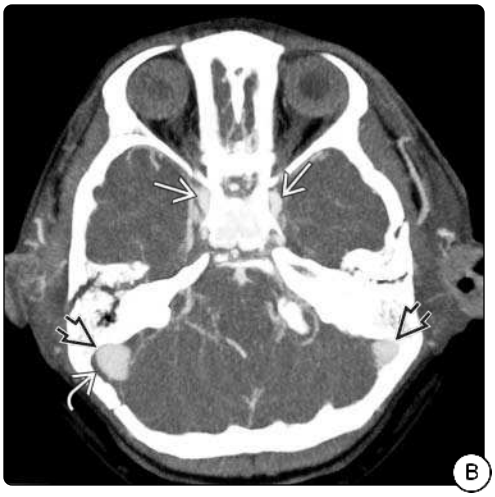

(2-15B) CT in the same case shows carotid arteries, sigmoid sinuses are patent. A small right venous EDH is present.

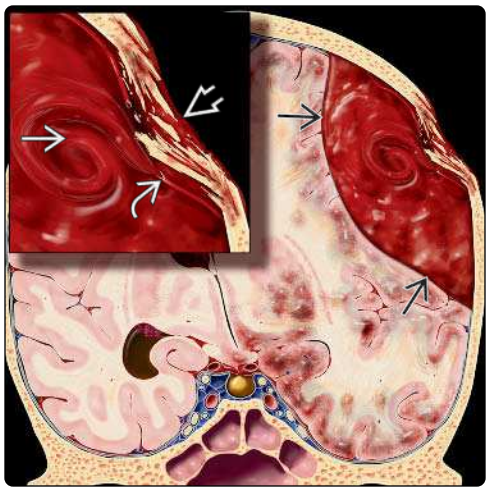

(2-16) Graphic shows EDH ⇨, depressed skull fracture ➡ lacerating middle meningeal artery ➡. Inset shows rapid bleeding, "swirl" sign ➡.

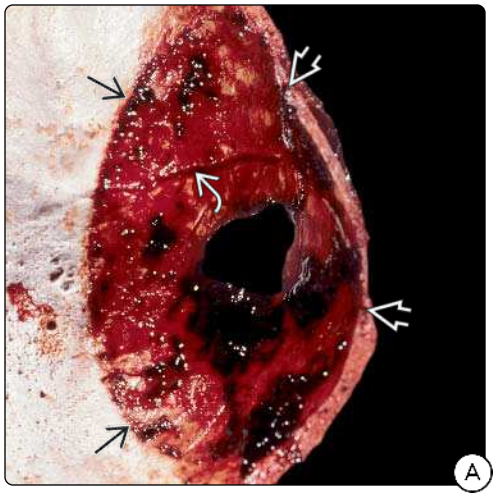

(2-17A) Endocranial view shows temporal bone fracture ➡ crossing the middle meningeal artery groove ➡. Note biconvex margins of EDH ⇨.

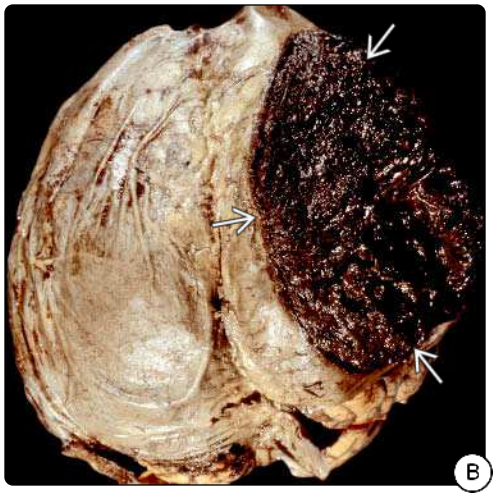

(2-17B) Dorsal view of the dura-covered brain shows the biconvex EDH ➡ on top of the dura. (Courtesy E. T. Hedley-Whyte, MD.)

MR Findings. MR is rarely used in the setting of acute head trauma because of high cost, limited availability, and lengthy time required. Compared with CT, bone detail is poor although parenchymal injuries are better seen. Adding T2* sequences, particularly SWI, is especially helpful in identifying hemorrhagic lesions.

In some cases, MR may be indicated for early detection of potentially treatable complications. A young child with neurologic deficits or seizures, a fracture larger than 4 millimeters, or a soft tissue mass extending through the fracture into the subgaleal space is at risk for developing a GSF. MR can demonstrate the dural tear and differentiate herniated brain from contused, edematous scalp.

Angiography. If a fracture crosses the site of a major vascular structure such as the carotid canal or a dural venous sinus **(2-14)**, CT angiography is recommended. Sagittal, coronal, and MIP reconstructions help delineate the site and extent of vascular injuries.

Clival and skull base fractures are strongly associated with neurovascular trauma, and CTA should always be obtained in these cases **(2-15)**. Cervical fracture dislocations, distraction injuries, and penetrating neck trauma also merit further investigation. Uncomplicated asymptomatic soft tissue injuries of the neck rarely result in significant vascular injury.

SCALP AND SKULL INJURIES

Scalp Injuries

- Lacerations
  - ± Foreign bodies
- Cephalohematoma
  - Usually infants
  - Subperiosteal
  - Small, unilateral (limited by sutures)
- Subgaleal hematoma
  - Between galea, periosteum of skull
  - Circumferential, not limited by sutures
  - Can be very large, life-threatening

Skull Fractures

- Linear
  - Sharp lucent line
  - Can be extensive and widespread
- Depressed
  - Focal
  - Inwardly displaced fragments
  - Often lacerates dura-arachnoid
- Elevated
  - Rare
  - Fragmented rotated outward
- Diastatic
  - Typically associated with severe trauma
  - Usually caused by linear fracture that extends into suture
  - Widens, spreads apart suture or synchondrosis
- "Growing"
  - Rare
  - Usually in young children
  - Fracture lacerates dura-arachnoid
  - Brain/arachnoid herniates through torn dura
  - Trapped tissue prevents bone healing
  - CT: Rounded edges, scalloped margins of skull
  - MR: CSF ± brain

Extraaxial Hemorrhages

Extraaxial hemorrhages and hematomas are common manifestations of head trauma. They can occur in any intracranial compartment, within any space (potential or actual), and between any layers of the cranial meninges. Only the subarachnoid spaces exist normally; all the other spaces are potential spaces and occur only under pathologic conditions.

Epidural hematomas arise between the inner table of the skull and outer (periosteal) layer of the dura. **Subdural hematomas** are located between the inner (meningeal) layer of the dura and the arachnoid. **Traumatic subarachnoid hemorrhage** is found within the sulci and subarachnoid cisterns, between the arachnoid and the pia.

To discuss extraaxial hemorrhages, we work our way from the outside to inside. We therefore begin this section with a discussion of epidural hematomas (both classic and variant), then move deeper inside the cranium to the more common subdural hematomas. We conclude with a consideration of traumatic subarachnoid hemorrhage.

Arterial Epidural Hematoma

Epidural hematomas (EDHs) are uncommon but potentially lethal complications of head trauma. If an EDH is promptly recognized and appropriately treated, mortality and morbidity can be minimized.

Terminology

An EDH is a collection of blood between the calvaria and outer (periosteal) layer of the dura.

Etiology

Most EDHs arise from direct trauma to the skull that lacerates an adjacent blood vessel **(2-16)**. The vast majority (90%) are caused by arterial injury, most commonly to the middle meningeal artery. Approximately 10% of EDHs are venous, usually secondary to a fracture that crosses a dural venous sinus (see below).

Pathology

Location. Over 90% of EDHs are unilateral and supratentorial. Between 90-95% are found directly adjacent to a skull fracture. The squamous portion of the temporal bone is the most common site.

Gross Pathology. EDHs are biconvex in shape **(2-17A)**. Adherence of the periosteal dura to the inner calvaria explains this typical configuration. As EDHs expand, they strip the dura away from the inner table of the skull, forming the classic lens-shaped hematoma **(2-17B)**. Because the dura is especially tightly attached to sutures, EDHs in adults rarely cross suture lines (10% of EDHs in children *do* cross sutures, especially if a fracture traverses the suture or sutural diastasis is present).

The typical gross or intraoperative appearance of an acute EDH is a dark purple ("currant jelly") lentiform clot.

Clinical Issues

Epidemiology. EDHs are much less common than either traumatic subarachnoid hemorrhage (tSAH) or subdural hematoma. Although EDHs represent up to 10% of fatal injuries in autopsy series, they are found in only 1-4% of patients imaged for craniocerebral trauma.

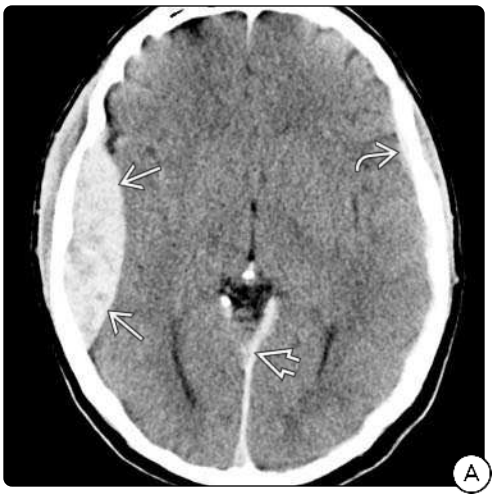

(2-18A) Biconvex aEDH is shown with a thin subdural blood collection along the tentorium, falx, and left hemisphere.

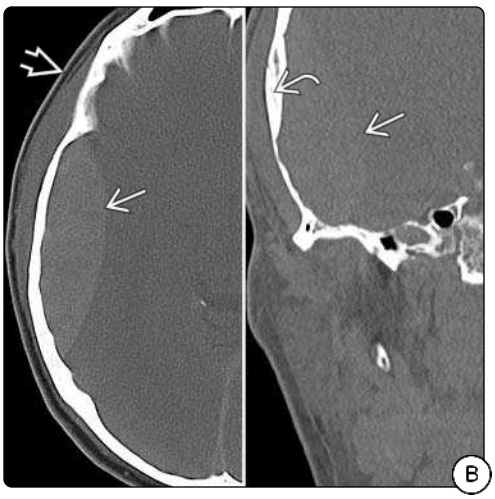

(2-18B) (L) Bone CT shows subgaleal hematoma, EDH. (R) Coronal bone CT demonstrates a subtle comminuted fracture.

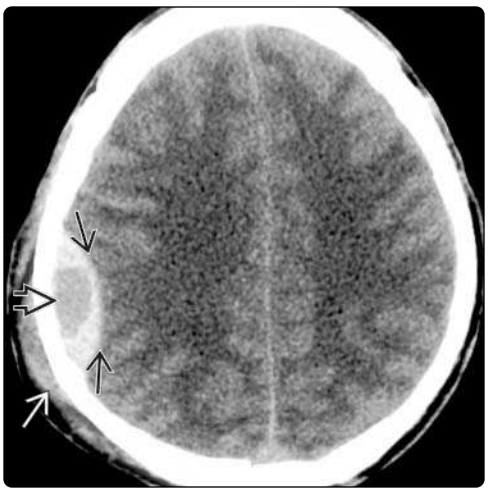

(2-19) Axial NECT shows an actively bleeding EDH with "swirl" sign, displaced cortex. A focal cephalohematoma is present.

(2-20A) Serial imaging demonstrates temporal evolution of a small nonoperated EDH. Initial NECT scan shows a hyperdense biconvex EDH ⇨.

(2-20B) Repeat scan 10 days later reveals that density of the EDH ⇨ has decreased significantly.

(2-20C) Repeat study 6 weeks after trauma reveals that the EDH has resolved completely.

Demographics. EDHs are uncommon in infants and the elderly. Most are found in older children and young adults. The M:F ratio is 4:1.

Presentation. The prototypical "lucid interval," during which a traumatized patient has an initial brief loss of consciousness followed by an asymptomatic period of various length prior to onset of coma and/or neurologic deficit, occurs in only 50% of EDH cases. Headache, nausea, vomiting, symptoms of intracranial mass effect (e.g., pupil-involving third cranial nerve palsy) followed by somnolence and coma are common.

Natural History. Outcome depends on size and location of the hematoma, whether the EDH is arterial or venous, and whether there is active bleeding (see below). In the absence of other associated traumatic brain injuries, overall mortality rate with prompt recognition and appropriate treatment is under 5%.

Delayed development or enlargement of an EDH occurs in 10-15% of cases, usually within 24-36 hours following trauma.

Treatment Options. Many EDHs are now treated conservatively. Most traumatic EDHs are not surgical lesions at initial presentation, and the rate of conversion to surgery is low. Most venous and small classic hyperdense EDHs that do not exhibit a "swirl" sign and have minimal or no mass effect are managed conservatively with close clinical observation and follow-up imaging **(2-20)**. Significant clinical predictors of EDH progression requiring conversion to surgical therapy are coagulopathy and younger age.

Imaging

General Features. EDHs, especially in adults, typically do not cross sutures unless a fracture with sutural diastasis is present. In children, 10% of EDHs cross suture lines, usually the coronal or sphenosquamous suture.

Look for other comorbid lesions such as "contre-coup" injuries, tSAH, and secondary brain herniations, all of which are common findings in patients with EDHs.

CT Findings. NECT scan is the procedure of choice for initial imaging in patients with head injury. Both soft tissue and bone reconstruction algorithms should be obtained. Multiplanar reconstructions are especially useful in identifying vertex EDHs, which may be difficult to detect if only axial images are obtained.

The classic imaging appearance of **classic** (**arterial) EDHs** is a hyperdense (60-90 HU) biconvex extraaxial collection **(2-18)**. Presence of a hypodense component ("swirl" sign) is seen in about one-third of cases and indicates active, rapid bleeding with unretracted clot **(2-16) (2-19)**.

EDHs compress the underlying subarachnoid space and displace the cortex medially, "buckling" the gray-white matter interface inward.

Air in an EDH occurs in approximately 20% of cases and is usually—but not invariably—associated with a sinus or mastoid fracture.

Patients with mixed-density EDHs tend to present earlier than patients with hyperdense hematomas and have lower Glasgow Coma Scores (GCSs), larger hematoma volumes, and poorer prognosis.

Imaging findings associated with adverse clinical outcome are thickness > 1.5 cm, volume > 30 mL, pterional (lateral aspect of the middle cranial fossa) location, midline shift > 5 mm, and presence of a "swirl sign" within the hematoma on imaging.

MR Findings. Acute EDHs are typically isointense with underlying brain, especially on T1WI. The displaced dura can be identified as a displaced "black line" between the hematoma and the brain.

Angiography. DSA may show a lacerated middle meningeal artery with "tram-track" fistulization of contrast from the middle meningeal artery into the paired middle meningeal veins. Mass effect with displaced cortical arteries and veins is seen.

CLASSIC ACUTE EPIDURAL HEMATOMA

Terminology
- EDH = blood between skull, dura

Etiology
- Associated skull fracture in 90-95%
- Arterial 90%
  - Most often middle meningeal artery
- Venous 10%

Pathology
- Unilateral, supratentorial (> 90%)
- Dura stripped away from skull → biconvex hematoma
- Usually does not cross sutures (exception = children, 10%)
- Does cross sites of dural attachment

Clinical
- Rare (1-4% of head trauma)
- Older children, young adults most common
- M:F = 4:1
- Classic "lucid interval" in only 50%
- Delayed deterioration common
- Low mortality if recognized, treated
- Small EDHs
  - If minimal mass, no "swirl sign" often managed conservatively

Imaging
- Hyperdense lens-shaped
- "Swirl sign" (hypodensity) = rapid bleeding

Venous Epidural Hematoma

Not all EDHs are the same!! **Venous EDHs** are often smaller, are under lower pressure, and develop more slowly than their arterial counterparts. Most venous EDHs are caused by a skull fracture that crosses a dural venous sinus and therefore occur in the posterior fossa near the skull base (transverse/sigmoid sinus) **(2-21)** or the vertex of the brain (superior sagittal sinus). In contrast to their arterial counterparts, venous EDHs can "straddle" intracranial compartments, crossing both sutures and lines of dural attachment **(2-22)** and compressing or occluding the adjacent venous sinuses.

Venous EDHs can be subtle and easily overlooked. Coronal and sagittal reformatted images are key to the diagnosis and delineation of these variant EDHs **(2-23)**. Several anatomic subtypes of venous EDHs, each with different treatment implications and prognosis, are recognized.

Vertex EDH

"Vertex" EDHs are rare. Usually caused by a linear or diastatic fracture that crosses the superior sagittal sinus, they often accumulate over hours or even days with slow, subtle onset of symptoms **(2-24)**. "Vertex" hematomas can be subtle and are easily overlooked unless coronal and sagittal reformatted images are obtained.

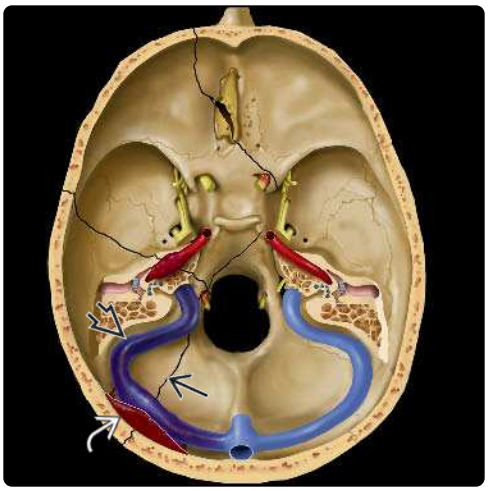

(2-21) Graphic shows basilar skull fracture ⇨ with transverse sinus occlusion ⇨ and posterior fossa venous EDH ⇨.

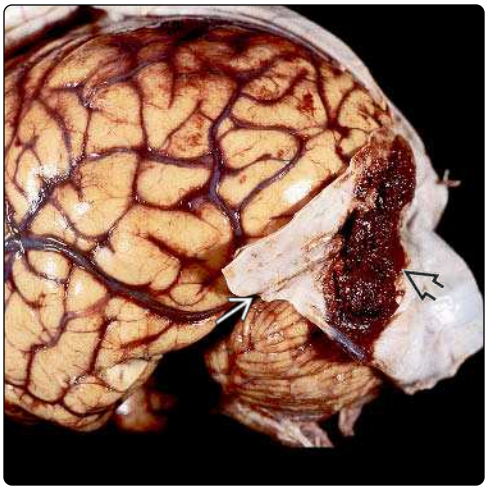

(2-22) Autopsy shows that venous EDH ⇨ caused by transverse sinus injury "straddles" the tentorium ⇨. (Courtesy R. Hewlett, MD.)

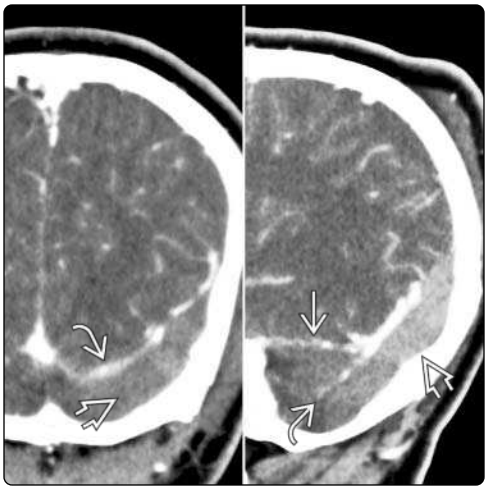

(2-23) (L) Coronal, (R) sagittal CTV shows venous EDH ⇨ straddling the tentorium ⇨, elevating the left transverse sinus ⇨.

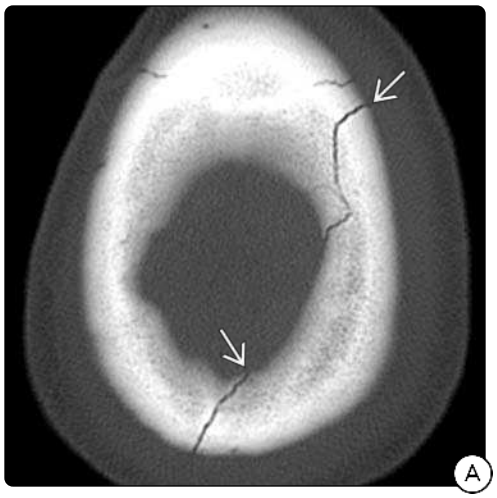

(2-24A) Bone CT in a 57y man shows a linear skull fracture that crosses the midline. No other abnormalities were present.

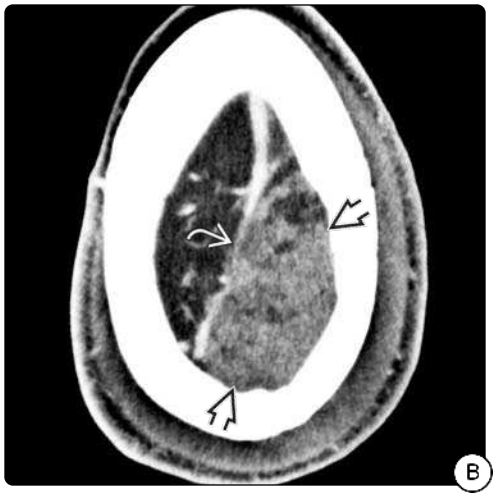

(2-24B) CT venogram after the patient deteriorated shows a large venous EDH. The middle SSS is compressed and thrombosed.

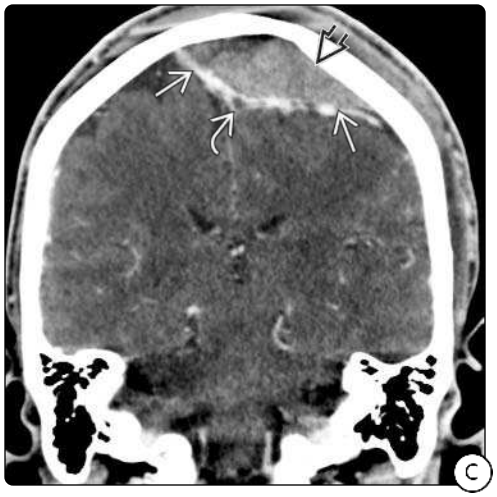

(2-24C) Coronal scan shows a vertex venous EDH crossing the midline. The thrombosed SSS, cortical veins are displaced inferiorly.

Anterior Temporal EDH

Anterior temporal EDHs are a unique subgroup of hematomas that occur in the anterior tip of the middle cranial fossa. Anterior temporal EDHs are caused either by an isolated fracture of the adjacent greater sphenoid wing or by an isolated zygomaticomaxillary complex ("tripod") facial fracture. The sphenoparietal dural venous sinus is injured as it curves medially along the undersurface of the lesser sphenoid wing, extravasating blood into the epidural space. Limited anatomically by the sphenotemporal suture laterally and the orbital fissure medially, anterior temporal EDHs remain stable in size and do not require surgical evacuation **(2-25)** **(2-26)**.

Clival EDH

Clival EDHs usually develop after a hyperflexion or hyperextension injury to the neck and are possibly caused by stripping of the tectorial membrane from attachments to the clivus. Less commonly, they have been associated with basilar skull fractures that lacerate the clival dural venous plexus.

Clival EDHs most often occur in children and present with multiple cranial neuropathies. The abducens nerve is the most commonly affected, followed by the glossopharyngeal and hypoglossal nerves. They are typically limited in size by the tight attachment of the dura to the basisphenoid and tectorial membrane **(2-27)**.

VENOUS EPIDURAL HEMATOMA

Not all EDHs are the same!
- Different etiologies in different anatomic locations
- Prognosis, treatment vary

Venous EDHs = 10% of all EDHs
- Skull fracture crosses dural venous sinus
  - Can cross sutures, dural attachments
- Often subtle, easily overlooked
  - Coronal, sagittal reformatted images key to diagnosis
- Usually accumulate slowly
- Can be limited in size; often treated conservatively

Subtypes
- Vertex EDH
  - Skull fracture crosses superior sagittal sinus (SSS)
  - SSS can be lacerated, compressed, thrombosed
  - Hematoma under low pressure, develops gradually
  - Slow onset of symptoms
  - May become large, cause significant mass effect
- Anterior temporal EDH
  - Sphenoid wing or zygomaticomaxillary fracture
  - Injures sphenoparietal venous sinus
  - Hematoma accumulates at anterior tip of middle cranial fossa
  - Limited anatomically (laterally by sphenotemporal suture, medially by orbital fissure)
  - Benign clinical course
- Clival EDH
  - Most common = child with neck injury
  - May cause multiple cranial neuropathies (CN VI most common)
  - Hyperdense collection under clival dura
  - Limited by tight attachment of dura to basisphenoid, tectorial membrane
  - Usually benign course, resolves spontaneously

Management of a clival EDH is dictated by severity and progression of the neurologic deficits and stability of the atlantoaxial joint. In patients with

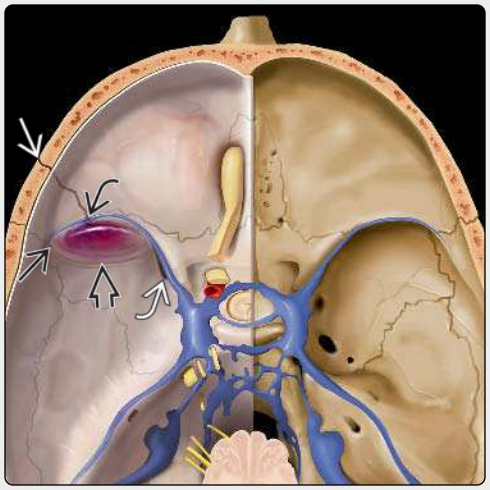

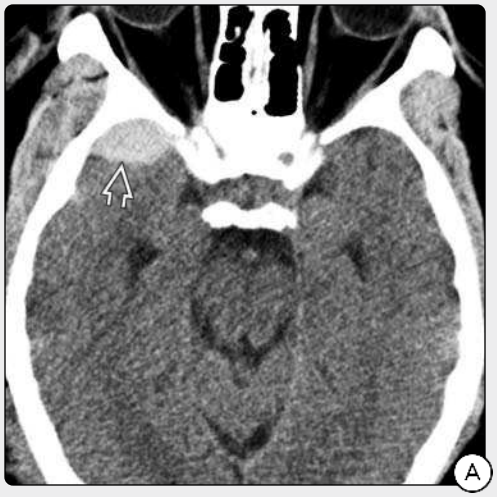

(2-25) *Graphic depicts benign anterior temporal epidural hematoma. Fracture ➡ disrupts the sphenoparietal sinus ⇨. Low-pressure venous EDH ⇨ is anatomically limited, medially by the orbital fissure ➡ and laterally by the sphenotemporal suture ⇨.* ***(2-26A)*** *Axial NECT in a 33y man with head trauma shows a biconvex anterior temporal acute epidural hematoma ➡.*

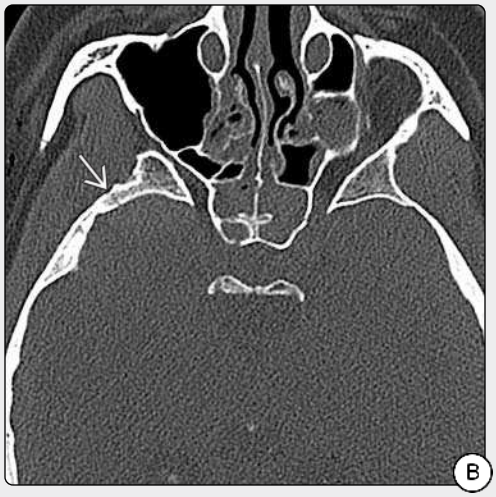

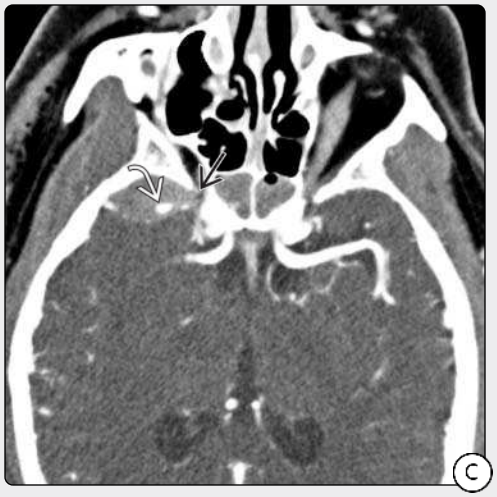

(2-26B) *Axial bone CT in the same case shows a fracture through the right greater sphenoid wing ➡.* ***(2-26C)*** *CT venogram in the same case shows a displaced, lacerated sphenoparietal sinus with contrast extravasation ("spot sign") ⇨. Note the EDH is limited medially by the orbital fissure ⇨. The patient was treated nonsurgically. The EDH showed no further enlargement and resolved completely.*

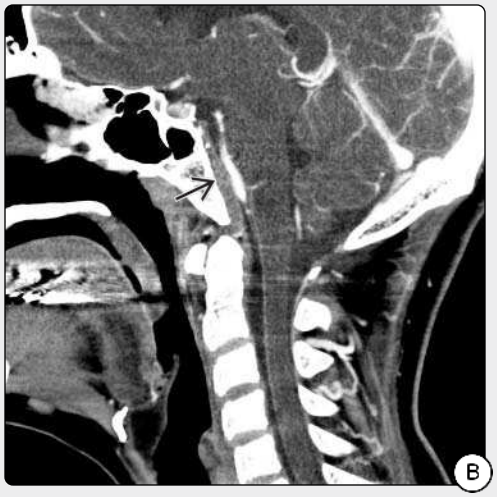

(2-27A) *Axial CTA in a child with craniovertebral junction trauma shows a small clival EDH ⇨. There was no evidence for vascular injury.* ***(2-27B)*** *Sagittal CTA reformatted from the axial source date nicely demonstrates the clival epidural hematoma ⇨.*

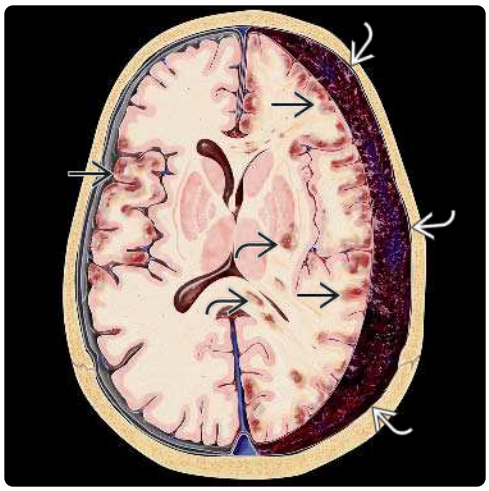

(2-28) Graphic depicts crescent-shaped acute SDH ➡ with contusions and "contre-coup" injuries ⇨, diffuse axonal injuries ⇨.

(2-29) Acute SDH spreads over left hemisphere ➡, along tentorium ➡, into interhemispheric fissure ➡ but does not cross midline.

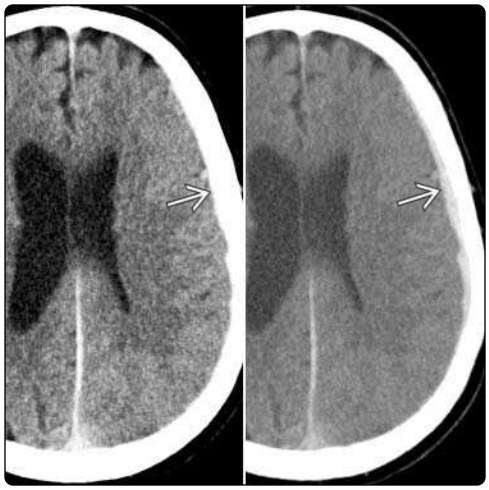

(2-30) NECT scan shows that small SDH ➡ is easier to see with wider (R) compared with standard (L) windows.

minor cranial nerve involvement, the clinical course is usually benign, and treatment with a cervical collar is typical.

NECT scans show a hyperdense collection between the clivus and tectorial membrane. Sagittal MR of the craniocervical junction shows the hematoma elevating the clival dura and extending inferiorly between the basisphenoid and tectorial membrane anterior to the medulla.

Acute Subdural Hematoma

Acute subdural hematomas (aSDHs) are one of the leading causes of death and disability in patients with severe traumatic brain injury. SDHs are much more common than EDHs. Most do not occur as isolated injuries; the vast majority of SDHs are associated with traumatic subarachnoid hemorrhage (tSAH) as well as significant parenchymal injuries such as cortical contusions, brain lacerations, and diffuse axonal injuries.

Terminology

An aSDH is a collection of acute blood products that lies in or between the inner border cell layer of the dura and the arachnoid **(2-28)**.

Etiology

Trauma is the most common cause of aSDH. Both direct blows to the head and nonimpact injuries may result in formation of an aSDH. Tearing of bridging cortical veins as they cross the subdural space to enter a dural venous sinus (usually the superior sagittal sinus) is the most common etiology. Cortical vein lacerations can occur with either a skull fracture or the sudden changes in velocity and brain rotation that occur during nonimpact closed head injury.

Blood from ruptured vessels spreads quickly through the potential space between the dura and the arachnoid. Large SDHs may spread over an entire hemisphere, extending into the interhemispheric fissure and along the tentorium.

Tearing of cortical arteries from a skull fracture may also give rise to an aSDH. The arachnoid itself may also tear, creating a pathway for leakage of CSF into the subdural space, resulting in admixture of both blood and CSF.

Less common causes of aSDH include aneurysm rupture, skull/dura-arachnoid metastases from vascular extracranial primary neoplasms, and spontaneous hemorrhage in patients with severe coagulopathy.

Rarely, an acute spontaneous SDH of arterial origin occurs in someone without any traumatic history or vascular anomaly. These patients usually have sudden serious disturbance of consciousness and have a poor outcome unless the aSDH is recognized and treated promptly.

Pathology

Gross Pathology. The gross appearance of an aSDH is that of a soft, purplish, "currant jelly" clot beneath a tense bulging dura. More than 95% are supratentorial. Most aSDHs spread diffusely over the affected hemisphere and are therefore typically crescent-shaped.

Clinical Issues

Epidemiology. An aSDH is the second most common extraaxial hematoma, exceeded only by tSAH. An aSDH is found in 10-20% of all patients with head injury and is observed in 30% of autopsied fatal injuries.

Demographics. An aSDH may occur at any age from infancy to the elderly. There is no sex predilection.

Presentation. Even relatively minor head trauma, especially in elderly patients who are often anticoagulated, may result in an aSDH. In such patients, a definite history of trauma may be lacking.

Clinical findings vary from none to loss of consciousness and coma. Most patients with aSDHs have low GCSs on admission. Delayed deterioration, especially in elderly anticoagulated patients, is common.

Natural History. An aSDH may remain stable, grow slowly, or rapidly increase in size, causing mass effect and secondary brain herniations. Prognosis varies with hematoma thickness, midline shift, and the presence of associated parenchymal injuries. An aSDH that is thicker than 2 centimeters correlates with poor outcome (35-90% mortality). An aSDH that occupies more than 10% of the total available intracranial volume is usually lethal.

Treatment Options. The majority of patients with small SDHs are initially treated conservatively with close clinical observation and follow-up imaging. Approximately 6-7% of these demonstrate an increase in SDH size over time and eventually require surgical intervention.

Patients with larger SDHs, a lesion located at the convexity, alcohol abuse, and repetitive falls are at the greatest risk for deterioration. Surveillance with follow-up CT scans is recommended until the SDH resolves or at least up to 5 weeks following the initial trauma.

Imaging

General Features. The classic finding of an aSDH is a supratentorial crescent-shaped extraaxial collection that displaces the gray-white matter interface medially. SDHs are typically more extensive than EDHs, easily spreading along the falx, tentorium, and around the anterior and middle fossa floors **(2-29)**. SDHs may cross suture lines but generally do not cross dural attachments. Bilateral SDHs occur in 15% of cases. "Contre-coup" injuries such as contusion of the contralateral hemisphere are common.

Both standard soft tissue and intermediate ("subdural") windows as well as bone algorithm reconstructions should be used in all trauma patients, as small, subtle aSDHs can be obscured by the density of the overlying calvaria **(2-30)**. Coronal and sagittal reformatted images using the axial source date are especially helpful in visualizing small ("smear") peritentorial and parafalcine aSDHs **(2-31)** **(2-32)**.

CT Findings

NECT. Approximately 60% of aSDHs are hyperdense on NECT scans **(2-29)**. Mixed-attenuation lesions are found in 40% of cases. Pockets of hypodensity within a larger hyperdense aSDH usually indicate rapid bleeding **(2-33)** **(2-34)**. "Dots" or "lines" of CSF trapped within compressed, displaced sulci are often seen underlying an aSDH.

Mass effect with an aSDH is common and expected. Subfalcine herniation should be proportionate to the size of the subdural collection. However, **if the difference between the midline shift and thickness of the hematoma is 3 mm or more, then mortality is very high.** This discrepancy occurs when underlying cerebral edema is triggered by the traumatic event. Early recognition and aggressive treatment for potentially catastrophic brain swelling are essential **(2-35)**.

In other cases, especially in patients with repeated head injury, severe brain swelling with unilateral hemisphere vascular engorgement occurs very

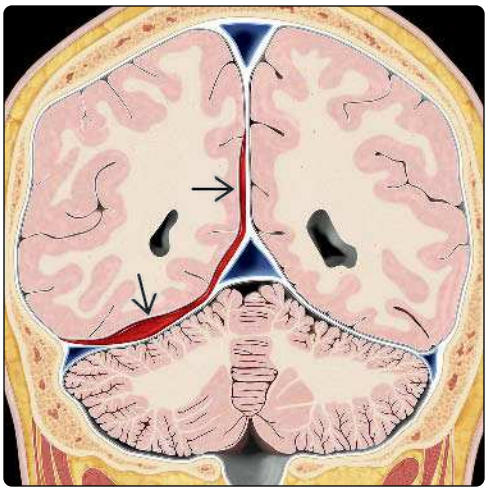

(2-31) Coronal graphic depicts thin aSDH layering along the tentorium and inferior falx cerebri.

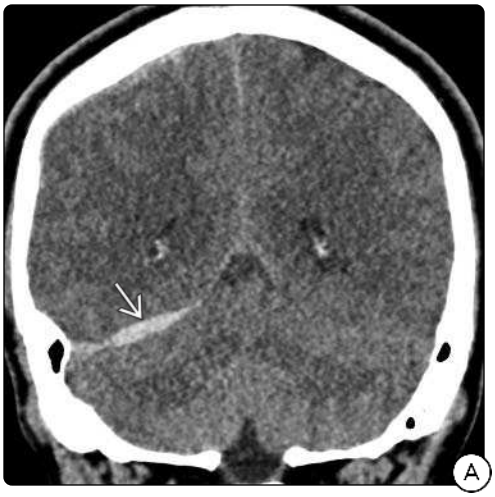

(2-32A) Reformatted coronal NECT scan using the axial source date shows a small right peritentorial aSDH.

(2-32B) Sagittal scans in the same case show the right peritentorial aSDH (top) with normal left sagittal dura (bottom) for comparison.

quickly. Here the mass effect is greatly disproportionate to the size of the SDH, which may be relatively small.

Occasionally, an aSDH is nearly isodense with the underlying cortex. This unusual appearance is found in extremely anemic patients (Hgb under 8-10 g/dL) **(2-36)** and sometimes occurs in patients with coagulopathy. In rare cases, CSF leakage through a torn arachnoid may mix with—and dilute—the acute blood that collects in the subdural space.

CECT. CECT scans are helpful in detecting small isodense aSDHs. The normally enhancing cortical veins are displaced inward by the extraaxial fluid collection.

Perfusion CT. CT or xenon perfusion scans may demonstrate decreased cerebral blood flow (CBF) and low perfusion pressure, which is one of the reasons for the high mortality rate of patients with aSDHs. The cortex underlying an evacuated aSDH may show hyperemic changes with elevated rCBF values. Persisting hyperemia has been associated with poor outcome.

MR Findings. MR scans are rarely obtained in acutely brain-injured patients. In such cases, aSDHs appear isointense on T1WI and hypointense on T2WI. Signal intensity on FLAIR scans is usually iso- to hyperintense compared with CSF but hypointense compared with the adjacent brain. aSDHs are hypointense on T2* scans.

DWI shows heterogeneous signal within the hematoma but may show patchy foci of restricted diffusion in the cortex underlying the aSDH.

Angiography. CTA may be useful in visualizing a cortical vessel that is actively bleeding into the subdural space.

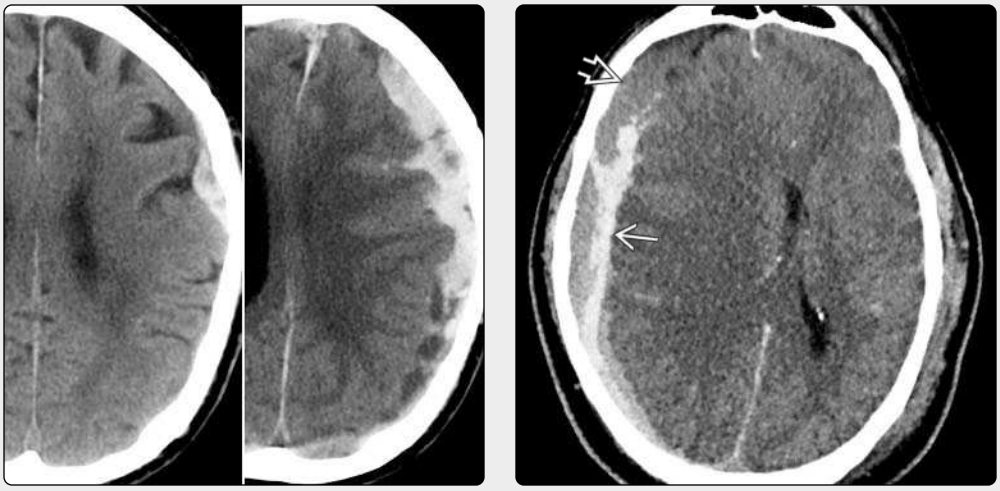

(2-33) (L) Initial NECT in an anticoagulated male patient shows a small mixed-density SDH. (R) Scan 6 hours later shows expanding, actively bleeding aSDH. (2-34) NECT scan shows a 55y man with an actively hemorrhaging aSDH. Some clotted blood is present ⇨, but much of the hematoma consists of isodense unclotted hemorrhage ⇨.

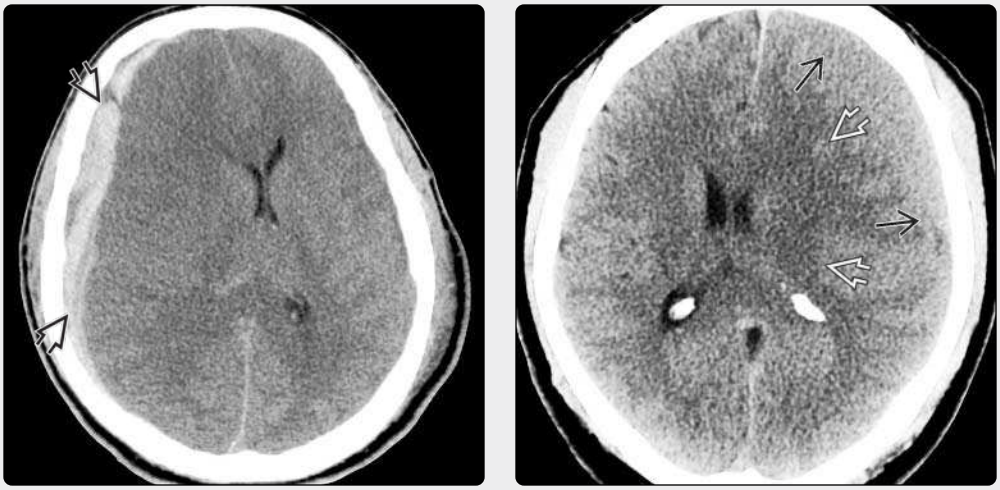

(2-35) NECT shows a mixed-density 12-mm aSDH ⇨ with a disproportionately large subfalcine herniation of the lateral ventricles (17 mm), indicating that diffuse holohemispheric brain swelling is present. Subfalcine herniation ≥ 3 mm portends a poor prognosis. (2-36) NECT scan in a very anemic patient shows an isodense aSDH ⇨. The aSDH is almost exactly the same density as the underlying cortex. The gray-white interface is displaced inward ⇨.

Differential Diagnosis

In the setting of acute trauma, the major differential diagnosis is EDH. Shape is a helpful feature, as most aSDHs are crescentic, whereas EDHs are biconvex. EDHs are almost always associated with skull fracture; SDHs frequently occur in the absence of skull fracture. EDHs may cross sites of dural attachment; SDHs do not cross the falx or tentorium.

Subacute Subdural Hematoma

With time, subdural hematomas (SDHs) undergo organization, lysis, and neomembrane formation. Within 2-3 days, the initial soft, loosely organized clot of an acute SDH becomes organized. Breakdown of blood products and the formation of organizing granulation tissue change the imaging appearance of subacute and chronic SDHs.

Terminology

A subacute subdural hematoma (sSDH) is between several days and several weeks old.

Pathology

A collection of partially liquified clot with resorbing blood products is surrounded on both sides by a "membrane" of organizing granulation tissue **(2-37)**. The outermost membrane adheres to the dura and is typically thicker than the inner membrane, which abuts the thin, delicate arachnoid **(2-38)**.

In some cases, repetitive hemorrhages of different ages arising from the friable granulation tissue may be present. In others, liquefaction of the hematoma over time produces serous blood-tinged fluid.

Clinical Issues

Epidemiology and Demographics. SDHs are common findings at imaging and autopsy. In contrast to acute SDHs, sSDHs show a distinct bimodal distribution with children and the elderly as the most commonly affected age groups.

Presentation. Clinical symptoms vary from asymptomatic to loss of consciousness and hemiparesis caused by sudden rehemorrhage into an sSDH. Headache and seizure are other common presentations.

Natural History and Treatment Options. Many sSDHs resolve spontaneously. In some cases, repeated hemorrhages may cause sudden enlargement and mass effect. Surgical drainage may be indicated if the sSDH is enlarging or becomes symptomatic.

Imaging

General Features. Imaging findings are related to hematoma age and the presence of encasing membranes. Evolution of an untreated, uncomplicated SDH follows a very predictable pattern on CT. Density of an extraaxial hematoma decreases approximately 1-2 HU each day **(2-39)**. Therefore, an SDH will become nearly isodense with the underlying cerebral cortex within a few days following trauma.

CT Findings. sSDHs are typically crescent-shaped fluid collections that are iso- to slightly hypodense compared with the underlying cortex on NECT **(2-40)**. Medial displacement of the gray-white interface ("buckling") is often present, along with "dot-like" foci of CSF in the trapped, partially effaced sulci underlying the sSDH **(2-41)** **(2-42)**. Mixed-density hemorrhages are common.

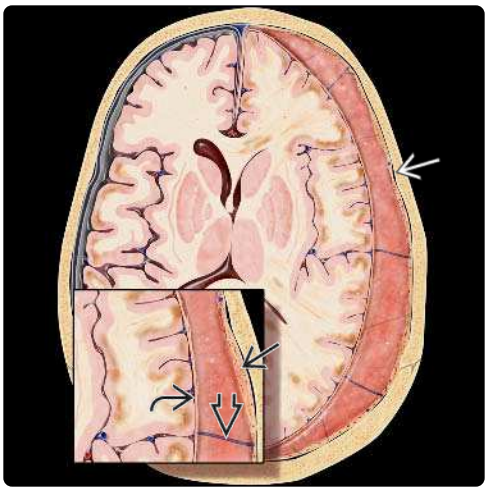

(2-37) Graphic depicts sSDH. Inset shows bridging vein and thin inner and thick outer membranes.

(2-38) Autopsy shows sSDH with organized hematoma, thick outer membrane, deformed brain. (Courtesy R. Hewlett, MD.)

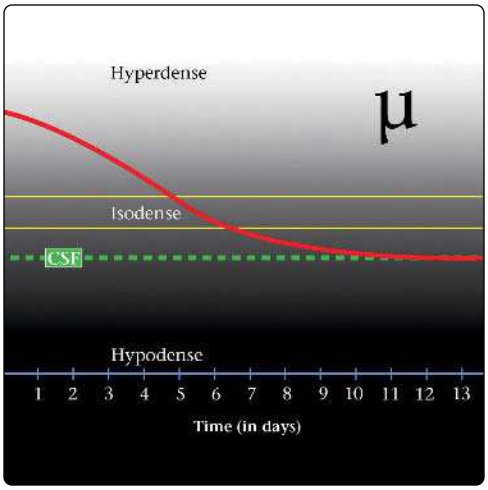

(2-39) SDHs decrease approximately 1.5 HU/day. By 7-10 days, blood in hematoma is isodense with cortex. By 10 days, it is hypodense.

***(2-40)** Axial NECT scan shows right sSDH ⇨ that is isodense with the underlying cortex. The right GM-WM interface is displaced and buckled medially ⇨ compared with normal left side ⇨. **(2-41)** NECT scan in another patient shows bilateral "balanced" isodense subacute SDHs ⇨. Note that both GM-WM interfaces are inwardly displaced. A "dot" of CSF in the compressed subarachnoid space is seen under the left sSDH ⇨.*

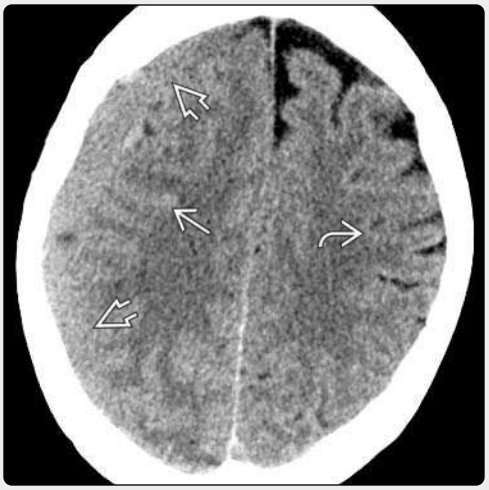

***(2-42)** NECT in elderly patient with sSDH, moderate cortical atrophy shows difference between nearly isodense SDH and CSF in underlying compressed subarachnoid space, sulci ⇨. **(2-43A)** Axial T1WI in patient with a late-stage aSDH shows crescent-shaped hyperintense collection ⇨ extending over entire surface of left hemisphere, gyral compression with almost obliterated sulci compared with normal right hemisphere.*

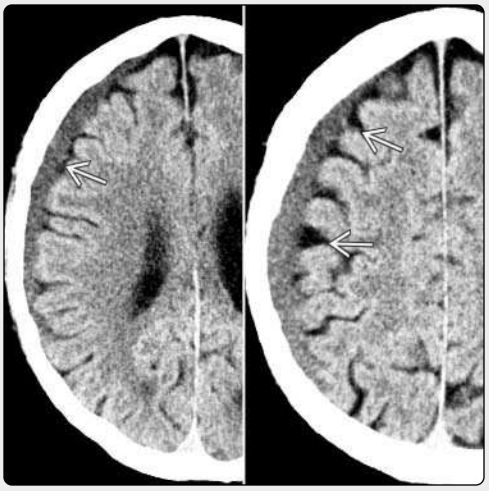

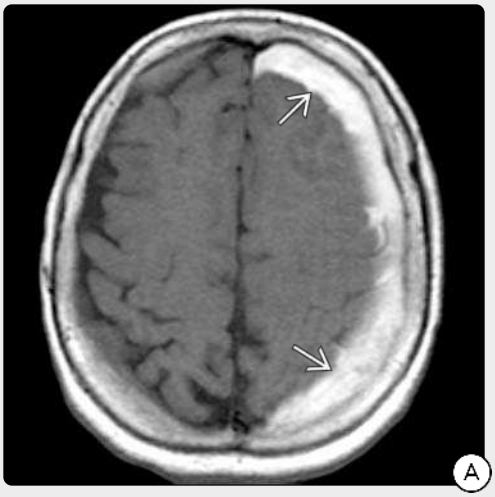

***(2-43B)** T2* GRE scan shows some "blooming" ⇨ in the sSDH. **(2-43C)** DWI shows the classic "double layer" appearance of an sSDH with hypointense rim on the inside ⇨ and mildly hyperintense rim on the outside ⇨ of the clot.*